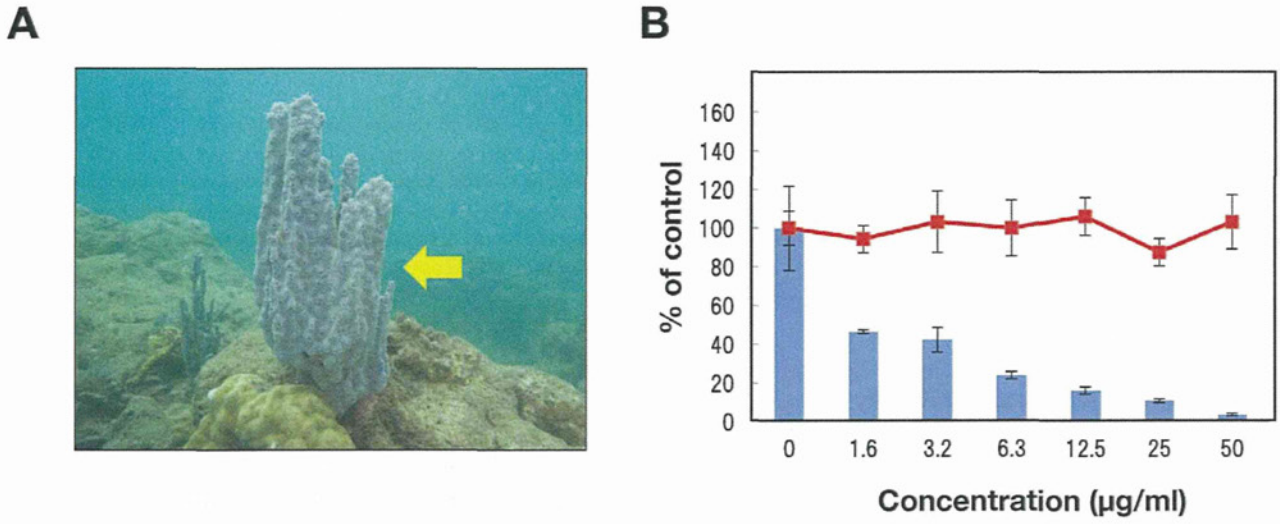

Figure 1. Effect of the extract prepared from a marine sponge on viral replication in the replicon cell line derived from viral genotype 1b. (A) *Amphimedon* sp. belongs to a marine sponge. The ethyl acetate fraction prepared from the marine organism was designated C-29EA in this study. (B) The Huh7 cell line, including the subgenomic replicon RNA of genotype 1b strain Con1, was incubated in medium containing various concentrations of C-29EA or DMSO (0). Luciferase and cytotoxicity assays were carried out as described in Materials and Methods. Error bars indicate standard deviation. The data represent three independent experiments.
doi:10.1371/journal.pone.0048685.g001

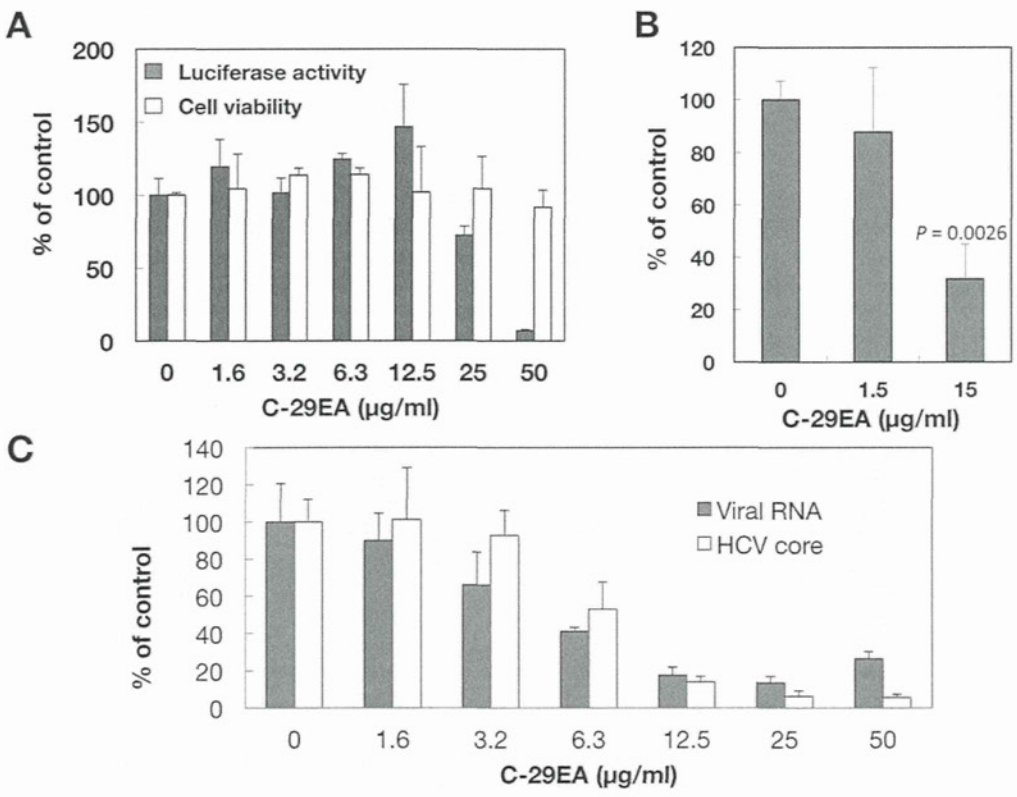

Figure 2. Effect of C-29EA extract on viral replication in the replicon cell line derived from viral genotype 2a. (A) The Huh7 cell line, including the subgenomic replicon RNA of genotype 2a strain JFH1, was incubated in medium containing various concentrations of C-29EA or DMSO (0). Luciferase and cytotoxicity assays were carried out as described in Materials and Methods. (B) The Huh7 OK1 cell line infected with HCVcc JFH1 was incubated with various concentrations of C-29EA or DMSO (0). The virus titers were determined by a focus-forming assay. The significance of differences in the means was determined by Student's *t*-test. (C) Amounts of viral RNA and core protein were estimated by qRT-PCR and ELISA, respectively. Error bars indicate standard deviation. The data represent three independent experiments. Treatment with DMSO corresponds to '0'.
doi:10.1371/journal.pone.0048685.g002

Table 2. Effect of C29EA on HCV replication.

HCV strain (genotype)	EC_{50} (μg/ml)[a]	CC_{50} (μg/ml)[b]	SI[c]
Con 1 (1b)	1.5	>50	>33.3
JFH1 (2a)	24.9	>50	>2.3

[a]: Fifty percent effective concentration based on the inhibition of HCV replication.
[b]: Fifty percent cytotoxicity concentration based on the reduction of cell viability.
[c]: SI, selectivity index (CC_{50}/EC_{50}).
doi:10.1371/journal.pone.0048685.t002

Effect of C-29EA on NS3 Protease Activity

Serine protease and helicase domains are respectively located on the N-terminal and C-terminal portions of NS3 [32]. Thus, we examined the effect of C-29EA on NS3 protease activity by using an NS3 protease assay based on FRET. NS3/4A serine protease was mixed with various concentrations of C-29EA. The initial velocity at each concentration of C-29EA was calculated during a 120 min reaction. The initial velocity in the absence of C-29EA represented 100% of relative protease activity. C-29EA decreased the serine protease activity in a dose-dependent manner (Fig. 7). The IC_{50} of C-29EA was 10.9 μg/ml, which is similar to the value estimated by helicase assay. These results suggest that C-29EA includes the compound(s) inhibiting the protease activity of NS3 in addition to the helicase activity.

Combination Antiviral Activity of C-29EA and Interferon-alpha

Treatment with C-29EA may potentiate inhibitory action of interferon-alpha, since it inhibited the protease and helicase activities of NS3 but not induce the interferon response as described above. Then, we examined effect of treatment using both interferon and C-29EA on HCV replication. The replication

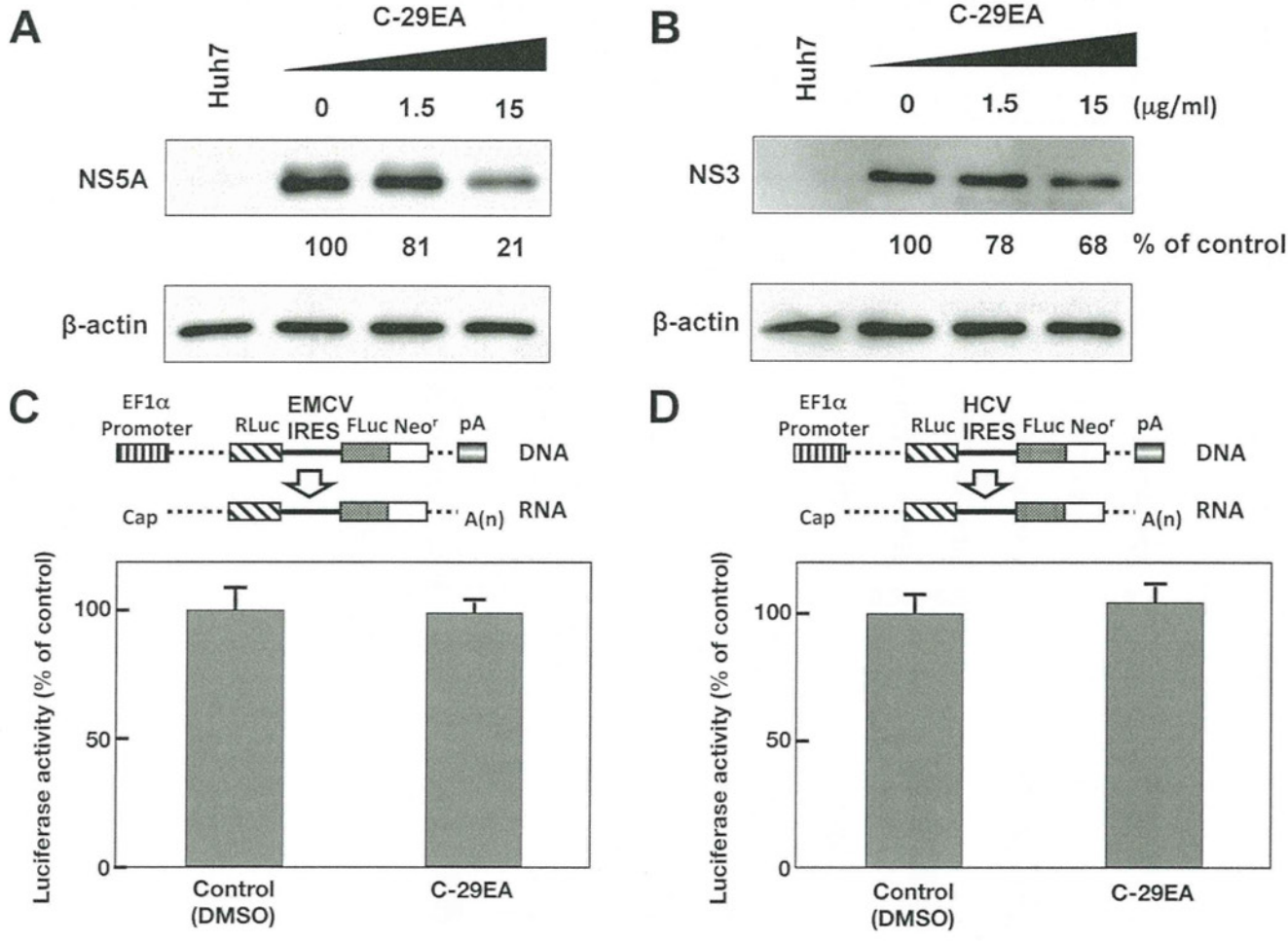

Figure 3. Effect of C-29EA on expression of viral proteins in replicon cell lines. The Huh7 replicon cell lines derived from genotype 1b (A) and 2a (B) were incubated with C-29EA at 37°C for 72 h. The treated cells were harvested and then subjected to Western blotting. Treatment with DMSO corresponds to '0'. The bicistronic gene is transcribed under the control of the elongation factor 1α (EF1α) promoter. The upstream cistron encoding *Renilla* luciferase (RLuc) is translated by a cap-dependent mechanism. The downstream cistron encodes the fusion protein (Feo), which consists of the firefly luciferase (Fluc) and neomycin phosphotransferase (Neo^r), and is translated under the control of the EMCV IRES (C) or HCV IRES (D). The Huh7 cell line transfected with the plasmid (each above the panel in C and D) was established in the presence of G418. The cells were incubated for 72 h without (control) and with 15 μg/ml of C-29EA. Firefly or *Renilla* luciferase activity was measured by the method described in Materials and Methods and was normalized by the protein concentration. F/R: relative ratio of firefly luciferase activity to *Renilla* luciferase activity. F/R is presented as a percentage of the control condition. Error bars indicate standard deviation. The data represent three independent experiments.
doi:10.1371/journal.pone.0048685.g003

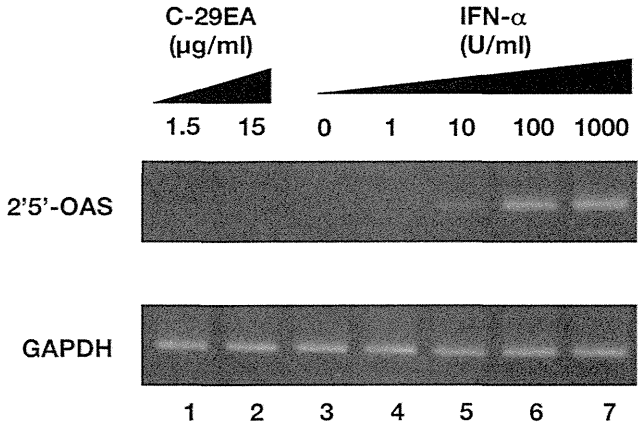

Figure 4. Effect of C-29EA on interferon signaling pathway. The Huh7 replicon cell line of genotype 1b was treated without (lane 3) or with 1, 10, 100, or 1000 U/mL interferon-alpha 2b (lanes 4–7), and 1.5 or 15 μg/ml C-29EA (lanes 1–2) for 48 h. Treatment with DMSO corresponds to '0'. The mRNAs of 2', 5'-OAS, and GAPDH as an internal control were detected by RT-PCR. Error bars indicate standard deviation. The data represent three independent experiments.
doi:10.1371/journal.pone.0048685.g004

of replicon was decreased in the presence of C-29EA or interferon-alpha and further decreased by combination treatment using interferon-alpha and C-29EA (Fig. 8A). Furthermore, we employed the isobologram method [33] to determine whether antiviral effect of the combination treatment exhibits additive or synergistic. EC_{90} values of interferon-alpha and C-29EA were estimated at 10.7 U/ml and 26.4 μg/ml, respectively, in the absence of each other. EC_{90} values of C-29EA in the presence of 0, 2.5 and 5 U/ml interferon-alpha were plotted to generate an isobole. Figure 8B shows that the isobole exhibits concave curvilinear, representing synergy but not additivity. These results suggest that combination treatment of interferon-alpha and C-29EA exhibits synergistic inhibition of HCV replication.

Discussion

Several natural products have been reported as anti-viral agents against HCV replication. Silbinin, epigallocatechin 3-gallate, and proanthocyanidins, which were prepared from milk thistle, green tea, and blueberry leaves, respectively, have exhibited inhibitory activity against HCV replication in cultured cells [34–37]. In our previous report, we identified manoalide as an anti-HCV agent from a marine sponge extract by high-throughput screening targeting NS3 helicase activity [38]. Manoalide inhibited ATPase, RNA binding, and NS3 helicase activity in enzymological assays. The EtOAc extract of the marine feather star also suppressed HCV replication in HCV replicon cell lines derived from genotype 1b, and it inhibited the RNA-binding activity but not the ATPase activity of NS3 helicase [30]. In this study, we screened 84 extracts of marine organisms for their ability to inhibit HCV replication in replicon cell lines and HCV cell culture system. Among these extracts, C-29EA, which was extracted from *Amphimedon* sp., most strongly inhibited HCV replication regardless of cytotoxicity. We previously reported that the EtOAc extract (SG1-23-1) of the feather star *Alloeocomatella polycladia* inhibited HCV replication with an EC_{50} of 22.9 to 44.2 μg/ml in HCV replicon cells derived from genotype 1b [30]. Treatment with C-29EA potently inhibited HCV replication with an EC_{50} of 1.5 μg/ml and with an SI of more than 33.3 in the replicon cell line derived from genotype 1b, regardless of cytotoxicity (Fig. 1B and Table 2). However, C-29EA exhibited an EC_{50} of 24.9 μg/ml in a replicon cell line derived from genotype 2a at a weaker level than in the replicon cell line derived from genotype 1b (Figs. 1 and 2), suggesting that the ability of C-29EA to suppress HCV replication is dependent on the viral genotype or strain.

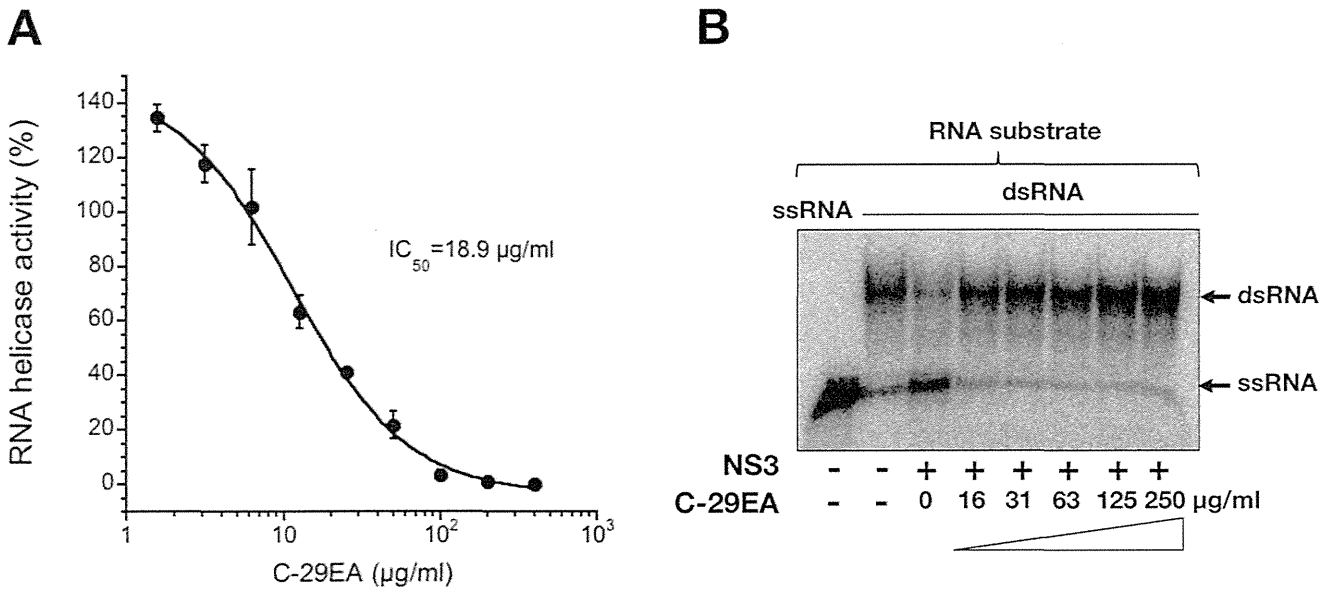

Figure 5. Effect of C-29EA on unwinding activity of NS3 helicase. (A) NS3 helicase activity was measured by PET assay. The reactions were carried out in the absence or presence of C-29EA. Helicase activity in the absence of C-29EA was defined as 100% helicase activity. Treatment with DMSO corresponds to '0'. The data are presented as the mean ± standard deviation for three replicates. (B) The unwinding activity of NS3 helicase was measured by an RNA unwinding assay using radioisotope-labeled RNA. The heat-denatured single-strand RNA (26-mer) and the partial duplex RNA substrate were applied to lanes 1 and 2, respectively. The duplex RNA was reacted with NS3 (300 nM) in the presence of C-29EA (lanes 4–9, 16–250 μg/ml). The resulting samples were subjected to native polyacrylamide gel electrophoresis. Treatment with DMSO corresponds to '0'.
doi:10.1371/journal.pone.0048685.g005

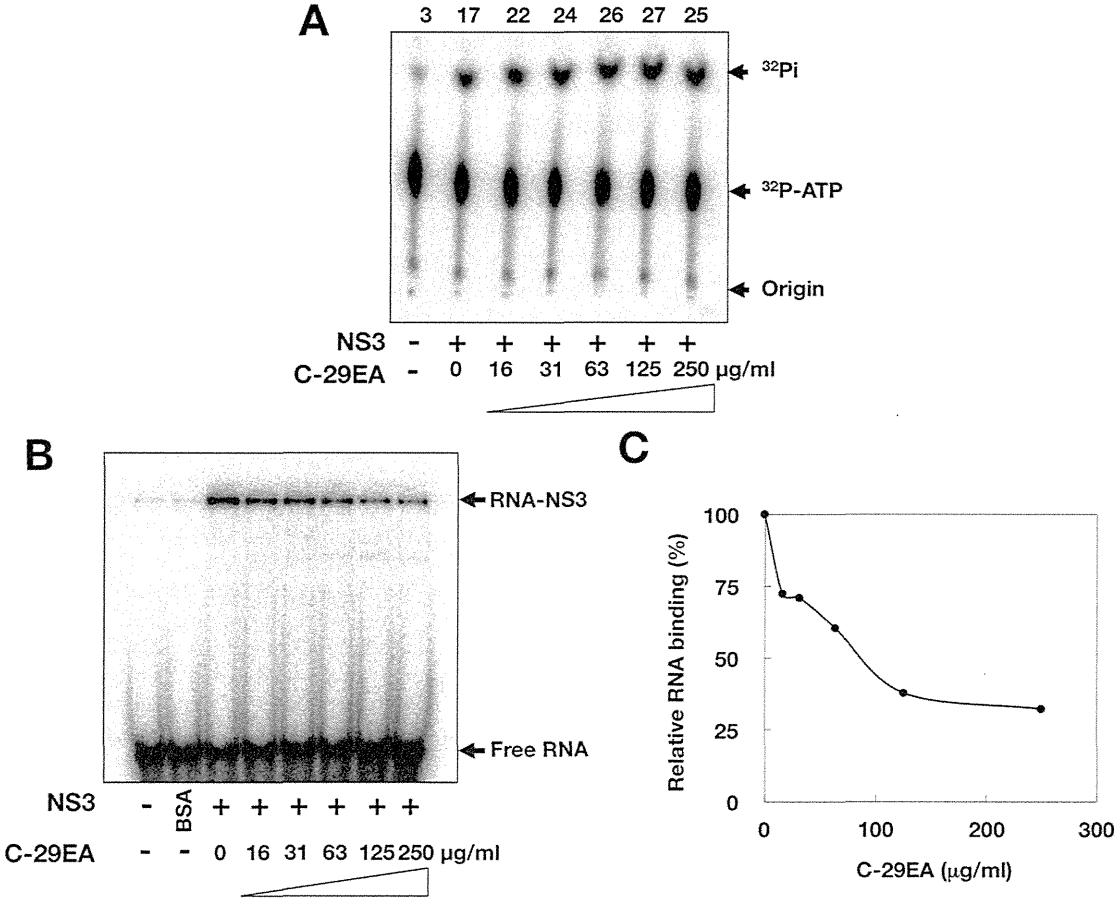

Figure 6. Effect of C-29EA on ATPase and RNA-binding activities of NS3 helicase. (A) The reaction mixtures were incubated with [γ-^{32}P] ATP as described in Materials and Methods. The reaction mixtures were subjected to thin-layer chromatography. The start positions and migrated positions of ATP and free phosphoric acid are indicated as 'Origin', '^{32}P-ATP', and '^{32}P-Pi', respectively, on the right side of the figure. The data represent three independent experiments. Treatment with DMSO corresponds to '0'. (B) Gel mobility shift assay for RNA-binding activity of NS3 helicase. The reaction was carried out with 0.5 nM labeled ssRNA at the indicated concentrations of C-29EA or DMSO. The reaction mixture was subjected to gel mobility shift assay. (C) The relative RNA-binding ability was calculated with band densities in each lane and presented as a percentage of RNA-NS3 in the total density. The data represent three independent experiments. Treatment with DMSO corresponds to '0'.
doi:10.1371/journal.pone.0048685.g006

HCV NS3 is well known to play a crucial role in viral replication through helicase and protease activities [5,39]. The N-terminal third of NS3 is responsible for serine protease activity in order to process the C-terminal portion of polyprotein containing viral nonstructural proteins [32]. The remaining portion of NS3 exhibits ATPase and RNA-binding activities responsible for helicase activity, which is involved in unwinding double-stranded RNA during replication of genomic viral RNA [40–42]. A negative-strand RNA is synthesized based on a viral genome (positive strand) after viral particles in the infected cells are uncoated, and is then used itself as a template to synthesize a positive-stranded RNA, which is translated or packaged into viral particles. Thus, both helicase and protease activities of NS3 are critical for HCV replication and could be targeted for the development of antiviral agents against HCV.

NS3 helicase activity was inhibited by treatment with C-29EA in a dose-dependent manner with an IC_{50} of 18.9 μg/ml (Fig. 5A). RNA-binding activity, but not ATPase activity, was inhibited by treatment with C-29EA (Fig. 6). Treatment with C-29EA did not significantly affect the HCV-IRES activity and did not induce interferon-stimulated gene 2′,5′-OAS (Figs. 3 and 4). Furthermore, the serine protease activity of NS3 was inhibited by using C-29EA with an IC_{50} of 10.9 μg/ml (Fig. 7). These results suggest that *Amphimedon* sp. includes the unknown compound(s) that could suppress NS3 enzymatic activity to inhibit HCV replication. Although the mechanism by which treatment with C-29EA could inhibit HCV replication has not yet been revealed, the unknown compound(s) may be associated with the inhibition of NS3 protease and helicase, leading to the suppression of HCV replication. However, other effects of extract C-29EA on HCV replication could not be excluded in this study.

The compound 1-N, 4-N-bis [4-(1H-benzimidazol-2-yl)phenyl] benzene-1,4-dicarboxamide, which is designated as $(BIP)_2B$, was reported to be a potent and selective inhibitor of HCV NS3 helicase [43]. This compound competitively decreases the binding ability of HCV NS3 helicase to nucleic acids. The compound $(BIP)_2B$ inhibited RNA-induced stimulation of ATPase, although it did not directly affect the ATP hydrolysis activity of NS3 helicase. Thus, $(BIP)_2B$ could not affect ATPase activity without RNA or with a high concentration of RNA. Treatment with C-29EA inhibited helicase activity and viral replication but not ATPase activity (Figs. 1B, 2, 5, and 6). This extract suppressed the binding of RNA to helicase but exhibited no suppression of ATPase by NS3 helicase. Thus, the inhibitory action of extract C-29EA seems

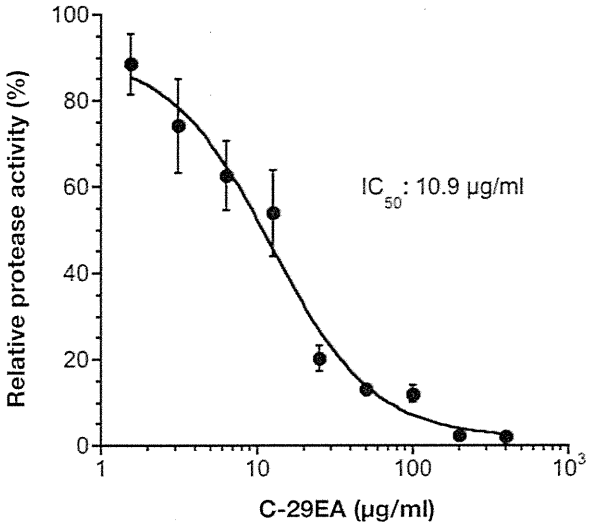

Figure 7. Effect of C-29EA on the activity of NS3 serine protease. NS3/4A serine protease was mixed with various concentrations of C-29EA or DMSO (0) in the reaction mixture and then incubated at 37°C for 120 min. The initial velocity at each concentration of C-29EA was calculated during 120 min reaction. The initial velocity in the absence of C-29EA was defined as 100% of relative protease activity. The data are presented as the mean ± standard deviation for three replicates.
doi:10.1371/journal.pone.0048685.g007

different from that of $(BIP)_2B$. The quinolone derivative QU663 was reported to inhibit the unwinding activity of NS3 helicase by binding to an RNA-binding groove irrespective of its own ATPase activity [44]. The compound QU663 may competitively bind the RNA-binding site of NS3 but not affect ATPase activity, resulting in the inhibition of unwinding activity. In this study, treatment with C-29EA inhibited the RNA-binding activities of NS3 helicase but did not affect ATPase activity (Fig. 6). Furthermore, treatment with C-29EA suppressed the viral replication of HCV in an HCV cell culture system derived from several virus strains (Figs. 1 and 2, Table 2). The mechanism of C-29EA on the inhibition of NS3 helicase may be similar to that of compound QU663.

It is unknown whether one or several molecules included in C-29EA are critical for the inhibition of protease and helicase activities. The serine protease NS3/4A is one of the viral factors targeted for development into antiviral agents. Improvements in HCV therapy over the past several years have resulted in FDA approval of telaprevir (VX-950) [15,45] and boceprevir (SCH503034) [46,47]. Several studies suggest that the activities of NS3/4A protease and helicase in the full-length molecule enhance each other [48,49]. The NS3/4A protease has formed a complex with macrocyclic acylsulfonamide inhibitors [50,51]. Schiering et al. recently reported the structure of full-length NS3/4A in complex with a macrocyclic acylsulfonamide protease inhibitor [52], although the structure of full-length HCV NS3/4A in complex with a protease inhibitor has not been reported. The inhibitor binds to the active site of the protease, while the P4-capping and P2 moieties of the inhibitor are exposed toward the helicase interface and interact with both protease and helicase residues [52]. An unknown compound included in C-29EA might interact with both protease and helicase domains of NS3 to inhibit their activities. However, our data in this study have not excluded the possibility that several compounds included in C-29EA are related to the inhibition of protease and helicase of NS3/4A.

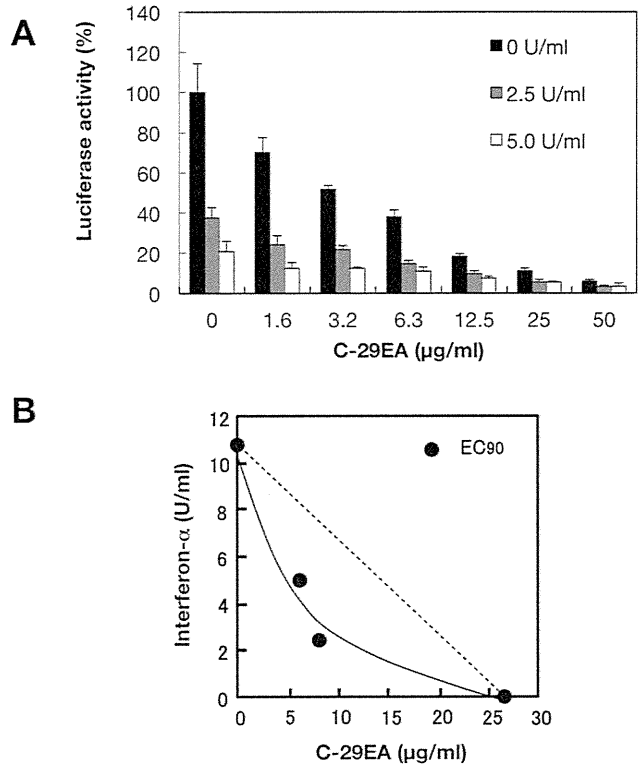

Figure 8. Effect of C-29EA on the antiviral activity of interferon-alpha. (A) The Huh7 cell line, including the subgenomic replicon RNA of genotype 1b strain Con1, was incubated in medium containing various concentrations of C-29EA or DMSO (0) in the presence or the absence of interferon-alpha. Luciferase assay were carried out as described in Materials and Methods. Error bars indicate standard deviation. The data represent three independent experiments. (B) Isobole plots of 90% inhibition of HCV replication. The broken line indicates the additive effect in the isobologram.
doi:10.1371/journal.pone.0048685.g008

In conclusion, we showed that the EtOAc extract from *Amphimedon* sp. significantly inhibits HCV replication by suppressing viral helicase and protease activities. The purification of an inhibitory compound from the extract of *Amphimedon* sp. will be necessary in order to improve its efficacy by chemical modification.

Materials and Methods

Preparation of Extracts from Marine Organisms

All marine organisms used in this study were hand-collected by scuba diving off islands in Okinawa Prefecture, Japan. No specific permits were required for the described field studies. We do not have to obtain a local government permit to collect invertebrates except for stony corals and marine organisms for fisheries, which we did not collect in this study. The areas where we collected are not privately-owned or protected in any way. We did not collect any invertebrates listed in the red data book issued by Ministry of Environment, Japan. The sponges, tunicates, and soft corals used in this study are not listed at all. Hence, no specific permits are required for this collection in the same way as the previous report of Aratake et al. [53].

The sponge from which C-29EA was extracted was identified as *Amphimedon* sp. and deposited at Naturalis under the code RMNH POR 6100. Each specimen was soaked in acetone. The acetone-extract fraction prepared from each specimen was concentrated.

The resulting material was fractionated as an EtOAc- and water-soluble fraction. The water-soluble fraction was dried up and solubilized in MeOH. The EtOAc- and the MeOH-soluble fractions were used for screening. All samples were dried and then solubilized in dimethyl sulfoxide (DMSO) before testing.

Cell Lines and Virus

The following Huh-7-derived cell lines used in this study were maintained in Dulbecco's modified Eagle's medium containing 10% fetal calf serum and 0.5 mg/ml G418. The Lunet/Con1 LUN Sb #26 cell line, which harbors the subgenomic replicon RNA of the Con1 strain (genotype 1b), was kindly provided by Ralf Bartenschlager [26]. Huh7/ORN3-5B #24 cell line, which harbors the subgenomic replicon RNA of the O strain (genotype 1b) was reported previously [54] and used for screening in this study (Table 1). HCV replicon cell line derived from genotype 2a strain JFH1 was described previously [55]. The surviving cells were infected with the JFH-1 virus at a multiplicity of infection (moi) of 0.05. The viral RNA derived from the plasmid pJFH1 was transcribed and introduced into Huh7OK1 cells according to the method of Wakita et al. [56]. The infectivity of the JFH1 strain was determined by a focus-forming assay [56].

Quantitative Reverse-transcription PCR (qRT-PCR) and Estimation of Core Protein

The estimation of viral RNA genome was carried out by the method described previously [57] with slight modification. Total RNAs were prepared from cells and culture supernatants by using an RNeasy mini kit (QIAGEN, Tokyo, Japan) and QIAamp Viral RNA mini kit (QIAGEN), respectively. First-strand cDNA was synthesized by using a high capacity cDNA reverse transcription kit (Applied Biosystems, Carlsbad, CA, USA) with random primers. Each cDNA was estimated by using Platinum SYBR Green qPCR SuperMix UDG (Invitrogen, Carlsbad, CA, USA) according to the manufacturer's protocol. Fluorescent signals of SYBR Green were analyzed by using an ABI PRISM 7000 (Applied Biosystems). The HCV internal ribosomal entry site (IRES) region was amplified using the primer pair 5′-GAGTGTCGTGCAGCCTCCA -3′ and 5′- CACTCGCAAG-CACCCTATCA -3′. Expression of HCV core protein was determined by an enzyme-linked immunosorbent assay (ELISA) as described previously [57].

Determination of Luciferase Activity and Cytotoxicity in HCV Replicon Cells

HCV replicon cells were seeded at 2×10^4 cells per well in a 48-well plate 24 h before treatment. C-29EA was added to the culture medium at various concentrations. The treated cells were harvested 72 h post-treatment and lysed in cell culture lysis reagent (Promega, Madison, WI, USA) or *Renilla* luciferase assay lysis buffer (Promega). Luciferase activity in the harvested cells was estimated with a luciferase assay system (Promega) or a *Renilla* luciferase assay system (Promega). The resulting luminescence was detected by the Luminescencer-JNR AB-2100 (ATTO, Tokyo, Japan) and corresponded to the expression level of the HCV replicon. Cell viability was measured by a dimethylthiazol carboxymethoxy-phenylsulfophenyl tetrazolium (MTS) assay using a CellTiter 96 aqueous one-solution cell proliferation assay kit (Promega).

Effects on Activities of Internal Ribosome Entry Site (IRES)

Huh7 cells were transfected with pEF.Rluc.HCV.IRES.Feo or pEF.Rluc.EMCV.IRES.Feo and then were established in medium containing 0.25 mg/ml G418, as described previously [58]. These cell lines were seeded at 2×10^4 cells per well in a 48-well plate 24 h before treatment, treated with 15 μg/ml extract C-29EA, and then harvested at 72 h post-treatment. The firefly luciferase activities were measured with a luciferase assay system (Promega). The total protein concentration was measured using the BCA Protein Assay Reagent Kit (Thermo Scientific, Rockford, IL, USA) to normalize luciferase activity.

Western Blotting and Reverse-transcription Polymerase Chain Reaction (RT-PCR)

Western blotting was carried out by a method described previously [30]. The antibodies to NS3 (clone 8G-2, mouse monoclonal, Abcam, Cambridge, UK), NS5A (clone 256-A, mouse monoclonal, ViroGen, Watertown, MA, USA), and beta-actin were purchased from Cell Signaling Technology (rabbit polyclonal, Danvers, MA, USA) and were used as the primary antibodies in this study. RT-PCR was carried out by a method described previously [30,58].

Assays for RNA Helicase, ATPase, and RNA-binding Activities

A continuous fluorescence assay based on photoinduced electron transfer (PET) was described previously [29] and was slightly modified with regard to the reaction mixture [30]. The NS3 RNA unwinding assay was carried out by the method of Gallinari et al. [59] with slight modifications [30]. NS3 ATPase activity was determined by the method of Gallinari et al. [59] with slight modifications [30]. RNA binding to NS3 helicase was analyzed by a gel mobility shift assay [30,31]. The gene encoding NS3 helicase was amplified from the viral genome of genotype 1b and was introduced into a plasmid for the expression of a recombinant protein [38,60]. The radioactive band was visualized with the Image Reader FLA-9000 and quantified by Multi Gauge V 3.11 software.

NS3 Protease Assay

The fluorescence NS3 serine protease assay based on fluorescence resonance energy transfer (FRET) was carried out by the modified method using the SensoLyte^{TM} 520 HCV protease assay kit (AnaSpec, Fremont, CA, USA). In brief, NS3 protein with a two-fold excess of NS4A cofactor peptide (Pep4AK) was prepared in 1× assay buffer provided with the kit. HCV NS3/4A protease was mixed with increasing concentrations of C-29EA and incubated at 37°C for 15 min. The reaction was started by adding the 5-FAM/QXL 520 substrate to the reaction mixture containing 180 nM HCV NS3/4A protease and various concentrations (0–400 μg/ml) of C-29EA. The resulting mixture (20 μl) was incubated at 37°C for 120 min using a LightCycler 1.5 (Roche Diagnostics, Basel, Switzerland). The fluorescence intensity was recorded every minute for 120 min. The NS3 serine protease activity was calculated as the initial reaction velocity and presented as a percentage of relative activity to that of the control examined with DMSO solvent but not C-29EA, in the same way as described in the fluorescence helicase assay [29].

Analysis of Drug-drug Interaction

The effects of drug combinations were evaluated using the isobologram method [33]. Various doses of C-29EA and interferon-alpha on 90% inhibition of HCV replication were combined to generate an isoeffect curve (isobole) to determine drug–drug interaction. Concave, linear, and convex curves exhibit synergy, additivity, and antagonism, respectively.

Statistical Analysis

The results are expressed as the mean ± standard deviation. The significance of differences in the means was determined by Student's *t*-test.

Acknowledgments

We thank T. Wakita and R. Bartenschlager for kindly providing the virus, cell lines, and plasmids; and H. Kasai and I. Katoh for their helpful comments and discussions.

Author Contributions

Conceived and designed the experiments: MN MT YS ST NA NN AY JT KM. Performed the experiments: YF KAS AF YM OF HT AY. Analyzed the data: MI NK NS SM NE. Wrote the paper: YF AY JT KM. Collected marine organisms: JT. Identified the sponge: NJdV.

References

1. Baldo V, Baldovin T, Trivello R, Floreani A (2008) Epidemiology of HCV infection. Curr Pharm Des 14: 1646–1654.
2. Seeff LB (2002) Natural history of chronic hepatitis C. Hepatology 36: S35–46.
3. Moriishi K, Matsuura Y (2012) Exploitation of lipid components by viral and host proteins for hepatitis C virus infection. Front Microbiol 3: 54.
4. Tsukiyama-Kohara K, Iizuka N, Kohara M, Nomoto A (1992) Internal ribosome entry site within hepatitis C virus RNA. J Virol 66: 1476–1483.
5. Kim DW, Gwack Y, Han JH, Choe J (1995) C-terminal domain of the hepatitis C virus NS3 protein contains an RNA helicase activity. Biochem Biophys Res Commun 215: 160–166.
6. Kanai A, Tanabe K, Kohara M (1995) Poly(U) binding activity of hepatitis C virus NS3 protein, a putative RNA helicase. FEBS Lett 376: 221–224.
7. Manns MP, Wedemeyer H, Cornberg M (2006) Treating viral hepatitis C: efficacy, side effects, and complications. Gut 55: 1350–1359.
8. McHutchison JG, Everson GT, Gordon SC, Jacobson IM, Sulkowski M, et al. (2009) Telaprevir with peginterferon and ribavirin for chronic HCV genotype 1 infection. N Engl J Med 360: 1827–1838.
9. Zeuzem S, Hultcrantz R, Bourliere M, Goeser T, Marcellin P, et al. (2004) Peginterferon alfa-2b plus ribavirin for treatment of chronic hepatitis C in previously untreated patients infected with HCV genotypes 2 or 3. J Hepatol 40: 993–999.
10. Asselah T, Marcellin P (2011) New direct-acting antivirals' combination for the treatment of chronic hepatitis C. Liver Int 31 Suppl 1: 68–77.
11. Jazwinski AB, Muir AJ (2011) Direct-acting antiviral medications for chronic hepatitis C virus infection. Gastroenterol Hepatol (N Y) 7: 154–162.
12. Lange CM, Sarrazin C, Zeuzem S (2010) Review article: specifically targeted anti-viral therapy for hepatitis C - a new era in therapy. Aliment Pharmacol Ther 32: 14–28.
13. Hofmann WP, Zeuzem S (2011) A new standard of care for the treatment of chronic HCV infection. Nat Rev Gastroenterol Hepatol 8: 257–264.
14. Kwong AD, Kauffman RS, Hurter P, Mueller P (2011) Discovery and development of telaprevir: an NS3–4A protease inhibitor for treating genotype 1 chronic hepatitis C virus. Nat Biotechnol 29: 993–1003.
15. Jacobson IM, McHutchison JG, Dusheiko G, Di Bisceglie AM, Reddy KR, et al. (2011) Telaprevir for previously untreated chronic hepatitis C virus infection. N Engl J Med 364: 2405–2416.
16. Sarrazin C, Hezode C, Zeuzem S, Pawlotsky JM (2012) Antiviral strategies in hepatitis C virus infection. J Hepatol 56 Suppl 1: S88–100.
17. Chen ST, Wu PA (2012) Severe Cutaneous Eruptions on Telaprevir. J Hepatol 57: 470–472.
18. Kieffer TL, Kwong AD, Picchio GR (2010) Viral resistance to specifically targeted antiviral therapies for hepatitis C (STAT-Cs). J Antimicrob Chemother 65: 202–212.
19. Thompson AJ, McHutchison JG (2009) Antiviral resistance and specifically targeted therapy for HCV (STAT-C). J Viral Hepat 16: 377–387.
20. Chin YW, Balunas MJ, Chai HB, Kinghorn AD (2006) Drug discovery from natural sources. AAPS J 8: E239–253.
21. Koehn FE, Carter GT (2005) The evolving role of natural products in drug discovery. Nat Rev Drug Discov 4: 206–220.
22. Li JW, Vederas JC (2009) Drug discovery and natural products: end of an era or an endless frontier? Science 325: 161–165.
23. Donia M, Hamann MT (2003) Marine natural products and their potential applications as anti-infective agents. Lancet Infect Dis 3: 338–348.
24. Molinski TF, Dalisay DS, Lievens SL, Saludes JP (2009) Drug development from marine natural products. Nat Rev Drug Discov 8: 69–85.
25. Mayer AM, Glaser KB, Cuevas C, Jacobs RS, Kem W, et al. (2010) The odyssey of marine pharmaceuticals: a current pipeline perspective. Trends Pharmacol Sci 31: 255–265.
26. Frese M, Barth K, Kaul A, Lohmann V, Schwarzle V, et al. (2003) Hepatitis C virus RNA replication is resistant to tumour necrosis factor-alpha. J Gen Virol 84: 1253–1259.
27. Blight KJ, Kolykhalov AA, Rice CM (2000) Efficient initiation of HCV RNA replication in cell culture. Science 290: 1972–1974.
28. Guo JT, Bichko VV, Seeger C (2001) Effect of alpha interferon on the hepatitis C virus replicon. J Virol 75: 8516–8523.
29. Tani H, Akimitsu N, Fujita O, Matsuda Y, Miyata R, et al. (2009) High-throughput screening assay of hepatitis C virus helicase inhibitors using fluorescence-quenching phenomenon. Biochem Biophys Res Commun 379: 1054–1059.
30. Yamashita A, Salam KA, Furuta A, Matsuda Y, Fujita O, et al. (2012) Inhibition of hepatitis C virus replication and NS3 helicase by the extract of the feather star *Alloeocomatella polycladia*. Mar Drugs 10: 744–761.
31. Huang Y, Liu ZR (2002) The ATPase, RNA unwinding, and RNA binding activities of recombinant p68 RNA helicase. J Biol Chem 277: 12810–12815.
32. Failla C, Tomei L, De Francesco R (1994) Both NS3 and NS4A are required for proteolytic processing of hepatitis C virus nonstructural proteins. J Virol 68: 3753–3760.
33. Leu GZ, Lin TY, Hsu JT (2004) Anti-HCV activities of selective polyunsaturated fatty acids. Biochem Biophys Res Commun 318: 275–280.
34. Ahmed-Belkacem A, Ahnou N, Barbotte L, Wychowski C, Pallier C, et al. (2010) Silibinin and related compounds are direct inhibitors of hepatitis C virus RNA-dependent RNA polymerase. Gastroenterology 138: 1112–1122.
35. Ciesek S, von Hahn T, Colpitts CC, Schang LM, Friesland M, et al. (2011) The green tea polyphenol, epigallocatechin-3-gallate, inhibits hepatitis C virus entry. Hepatology 54: 1947–1955.
36. Takeshita M, Ishida Y, Akamatsu E, Ohmori Y, Sudoh M, et al. (2009) Proanthocyanidin from blueberry leaves suppresses expression of subgenomic hepatitis C virus RNA. J Biol Chem 284: 21165–21176.
37. Wagoner J, Negash A, Kane OJ, Martinez LE, Nahmias Y, et al. (2010) Multiple effects of silymarin on the hepatitis C virus lifecycle. Hepatology 51: 1912–1921.
38. Salam KA, Furuta A, Noda N, Tsuneda S, Sekiguchi Y, et al. (2012) Inhibition of Hepatitis C Virus NS3 Helicase by Manoalide. J Nat Prod 75: 650–654.
39. Bartenschlager R, Ahlborn-Laake L, Mous J, Jacobsen H (1993) Nonstructural protein 3 of the hepatitis C virus encodes a serine-type proteinase required for cleavage at the NS3/4 and NS4/5 junctions. J Virol 67: 3835–3844.
40. Belon CA, Frick DN (2009) Helicase inhibitors as specifically targeted antiviral therapy for hepatitis C. Future Virol 4: 277–293.
41. Frick DN (2007) The hepatitis C virus NS3 protein: a model RNA helicase and potential drug target. Curr Issues Mol Biol 9: 1–20.
42. Kwong AD, Rao BG, Jeang KT (2005) Viral and cellular RNA helicases as antiviral targets. Nat Rev Drug Discov 4: 845–853.
43. Belon CA, High YD, Lin TI, Pauwels F, Frick DN (2010) Mechanism and specificity of a symmetrical benzimidazolephenylcarboxamide helicase inhibitor. Biochemistry 49: 1822–1832.
44. Maga G, Gemma S, Fattorusso C, Locatelli GA, Butini S, et al. (2005) Specific targeting of hepatitis C virus NS3 RNA helicase. Discovery of the potent and selective competitive nucleotide-mimicking inhibitor QU663. Biochemistry 44: 9637–9644.
45. Reesink HW, Zeuzem S, Weegink CJ, Forestier N, van Vliet A, et al. (2006) Rapid decline of viral RNA in hepatitis C patients treated with VX-950: a phase Ib, placebo-controlled, randomized study. Gastroenterology 131: 997–1002.
46. Malcolm BA, Liu R, Lahser F, Agrawal S, Belanger B, et al. (2006) SCH 503034, a mechanism-based inhibitor of hepatitis C virus NS3 protease, suppresses polyprotein maturation and enhances the antiviral activity of alpha interferon in replicon cells. Antimicrob Agents Chemother 50: 1013–1020.
47. Njoroge FG, Chen KX, Shih NY, Piwinski JJ (2008) Challenges in modern drug discovery: a case study of boceprevir, an HCV protease inhibitor for the treatment of hepatitis C virus infection. Acc Chem Res 41: 50–59.
48. Beran RK, Pyle AM (2008) Hepatitis C viral NS3–4A protease activity is enhanced by the NS3 helicase. J Biol Chem 283: 29929–29937.
49. Beran RK, Serebrov V, Pyle AM (2007) The serine protease domain of hepatitis C viral NS3 activates RNA helicase activity by promoting the binding of RNA substrate. J Biol Chem 282: 34913–34920.
50. Cummings MD, Lindberg J, Lin TI, de Kock H, Lenz O, et al. (2010) Induced-fit binding of the macrocyclic noncovalent inhibitor TMC435 to its HCV NS3/NS4A protease target. Angew Chem Int Ed Engl 49: 1652–1655.
51. Romano KP, Ali A, Royer WE, Schiffer CA (2010) Drug resistance against HCV NS3/4A inhibitors is defined by the balance of substrate recognition versus inhibitor binding. Proc Natl Acad Sci U S A 107: 20986–20991.
52. Schiering N, D'Arcy A, Villard F, Simic O, Kamke M, et al. (2011) A macrocyclic HCV NS3/4A protease inhibitor interacts with protease and helicase residues in the complex with its full-length target. Proc Natl Acad Sci U S A 108: 21052–21056.

53. Aratake S, Tomura T, Saitoh S, Yokokura R, Kawanishi Y, et al. (2012) Soft coral Sarcophyton (Cnidaria: Anthozoa: Octocorallia) species diversity and chemotypes. PLoS One 7: e30410.
54. Ikeda M, Abe K, Dansako H, Nakamura T, Naka K, et al. (2005) Efficient replication of a full-length hepatitis C virus genome, strain O, in cell culture, and development of a luciferase reporter system. Biochem Biophys Res Commun 329: 1350–1359.
55. Nishimura-Sakurai Y, Sakamoto N, Mogushi K, Nagaie S, Nakagawa M, et al. (2010) Comparison of HCV-associated gene expression and cell signaling pathways in cells with or without HCV replicon and in replicon-cured cells. J Gastroenterol 45: 523–536.
56. Wakita T, Pietschmann T, Kato T, Date T, Miyamoto M, et al. (2005) Production of infectious hepatitis C virus in tissue culture from a cloned viral genome. Nat Med 11: 791–796.
57. Moriishi K, Shoji I, Mori Y, Suzuki R, Suzuki T, et al. (2010) Involvement of PA28gamma in the propagation of hepatitis C virus. Hepatology 52: 411–420.
58. Jin H, Yamashita A, Maekawa S, Yang P, He L, et al. (2008) Griseofulvin, an oral antifungal agent, suppresses hepatitis C virus replication in vitro. Hepatol Res 38: 909–918.
59. Gallinari P, Brennan D, Nardi C, Brunetti M, Tomei L, et al. (1998) Multiple enzymatic activities associated with recombinant NS3 protein of hepatitis C virus. J Virol 72: 6758–6769.
60. Nishikawa F, Funaji K, Fukuda K, Nishikawa S (2004) In vitro selection of RNA aptamers against the HCV NS3 helicase domain. Oligonucleotides 14: 114–129.

JOURNAL OF NATURAL PRODUCTS

Article

pubs.acs.org/jnp

Inhibition of Hepatitis C Virus NS3 Helicase by Manoalide

Kazi Abdus Salam,[†] Atsushi Furuta,[‡,§] Naohiro Noda,[‡,§] Satoshi Tsuneda,[‡] Yuji Sekiguchi,[§] Atsuya Yamashita,[⊥] Kohji Moriishi,[⊥] Masamichi Nakakoshi,[∥] Masayoshi Tsubuki,[∥] Hidenori Tani,[†] Junichi Tanaka,[▽] and Nobuyoshi Akimitsu[†,*]

[†]Radioisotope Center, The University of Tokyo, 2-11-16 Yayoi, Bunkyo-ku, Tokyo 113-0032, Japan

[‡]Department of Life Science and Medical Bio-Science, Waseda University, 2-2 Wakamatsu-cho, Shinjuku-ku, Tokyo 162-8480, Japan

[§]Biomedical Research Institute, National Institute of Advanced Industrial Science and Technology (AIST), 1-1-1 Higashi, Tsukuba, Ibaraki 305-8566, Japan

[⊥]Department of Microbiology, Graduate School of Medicine and Engineering, University of Yamanashi, 1110 Shimokato, Chuo-shi, Yamanashi 409-3898, Japan

[∥]Institute of Medical Chemistry, Hoshi University, Ebara 2-4-41, Shinagawa-ku, Tokyo 142-8501, Japan

[▽]Department of Chemistry, Biology and Marine Science, University of the Ryukyus, Nishihara, Okinawa 903-0213, Japan

Supporting Information

ABSTRACT: The hepatitis C virus (HCV) causes one of the most prevalent chronic infectious diseases in the world, hepatitis C, which ultimately develops into liver cancer through cirrhosis. The NS3 protein of HCV possesses nucleoside triphosphatase (NTPase) and RNA helicase activities. As both activities are essential for viral replication, NS3 is proposed as an ideal target for antiviral drug development. In this study, we identified manoalide (**1**) from marine sponge extracts as an RNA helicase inhibitor using a high-throughput screening photoinduced electron transfer (PET) system that we previously developed. Compound **1** inhibits the RNA helicase and ATPase activities of NS3 in a dose-dependent manner, with IC_{50} values of 15 and 70 μM, respectively. Biochemical kinetic analysis demonstrated that **1** does not affect the apparent K_m value (0.31 mM) of NS3 ATPase activity, suggesting that **1** acts as a noncompetitive inhibitor. The binding of NS3 to single-stranded RNA was inhibited by **1**. Manoalide (**1**) also has the ability to inhibit the ATPase activity of human DHX36/RHAU, a putative RNA helicase. Taken together, we conclude that **1** inhibits the ATPase, RNA binding, and helicase activities of NS3 by targeting the helicase core domain conserved in both HCV NS3 and DHX36/RHAU.

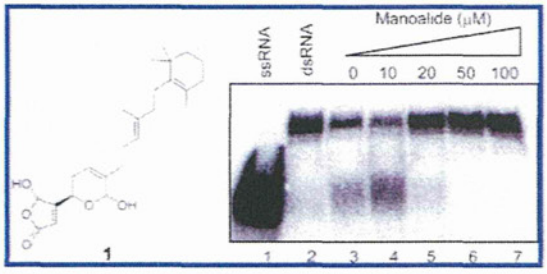

Hepatitis C is an infectious liver disease caused by the hepatitis C virus (HCV) that leads to liver fibrosis, cirrhosis, and finally hepatocellular carcinoma in 2−4% of all of cases.[1] Liver transplantation is the only chance of survival at late stage cirrhosis, resulting in significant increases in transplantations in many countries. More than 170 million people are infected with HCV, corresponding to 3% of the world's population, and 3 to 4 million people are infected each year.[2−4] Overall, HCV contributes to between 50% and 76% of all liver cancers and two-thirds of liver transplants in developed countries.[5] Today, HCV is one of the major global health issues.

Current therapy with pegylated interferon-α and ribavirin is the best choice, although it is only effective in approximately 50% of the patients. This combined therapy is expensive, is associated with serious side effects, and requires long-term administration.[6−8] Unfortunately, no vaccine is available due to the fact that HCV is rapidly mutable, allowing the virus to escape from the neutralizing antibodies, but attempts are continuing. Therefore, novel antiviral drugs are urgently needed.

HCV is a single-stranded positive sense RNA virus belonging to the family *Flaviviridae*[9,10] with seven genotypes and more than 50 subtypes. The viral genome comprises about 9.6 kb including a 5′-untranslated region (UTR) with an internal ribosomal entry site, an open reading frame encoding a single polyprotein of 3000 amino acids, and a 3′-UTR.[11] The polyprotein, in the sequence of C-E1-E2-p7-NS2-NS3-NS4A-NS4B-NS5A-NS5B, undergoes co- and post-translational cleavage by both viral and cellular proteases to form 10 individual proteins. The structural proteins C to E2 are involved in the formation of the viral capsid and envelope, while nonstructural proteins p7 to NS5B are responsible for viral replication. Among them, NS3 is a multifunctional protein of 631 amino acids and two domains. The N-terminal domain (aa 1−180) has serine protease activity, whereas the C-terminal

Received: November 8, 2011
Published: March 6, 2012

domain (aa 181–631) exhibits RNA helicase activity.[12,13] Like other helicases, NS3 helicase possesses NTPase (nucleoside triphosphatase) activity, which is essential for their translocation and unwinding of double-stranded RNA (dsRNA) in a 3′ to 5′ direction during replication of viral genomic RNA. Therefore, NTPase/helicases, such as the NS3 protease, are promising targets for developing directly acting antiviral chemotherapy.

Telaprevir and boceprevir are two NS3 protease inhibitors that were recently approved by the FDA for use as a triple therapy in combination with pegylated interferon-α and ribavirin for the treatment of chronic genotype 1 HCV infections.[14,15] This triple therapy improved the SVR (sustained virologic response) up to 70–80% of the current standard of care with minor adverse reactions: mainly rashes, anemia, and nausea. In contrast, no ideal RNA helicase inhibitor has been approved in clinical trials.

Manoalide (**1**) is a marine natural product, first isolated in the early 1980s from the sponge *Luffariella variabilis*.[16] It is a member of a chemical family known as the sesterterpenes. Although this natural product was originally reported as an antibiotic, follow-up work revealed that manoalide possesses promising anti-inflammatory properties.[17] Manaolide (**1**) was reported as the first marine natural product inhibiting the phospholipases A_2 (PLA_2s). PLA_2s play an important role in the inflammation process. To date **1** is the most investigated marine PLA_2 antagonist. It also inhibits calcium channels, 5-lipoxygenase, and phospholipase C.[18–20] No antiviral activity of **1** has been reported yet. In this study, we identified **1** by screening marine organism extracts and characterized its HCV NS3 helicase inhibitory activity. We found that **1** acts through the inhibition of NS3 ATPase activity and RNA binding.

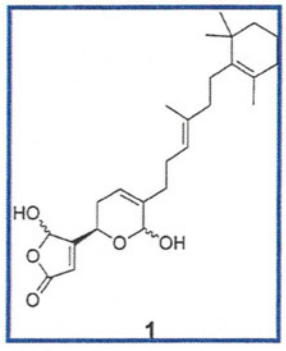

RESULTS AND DISCUSSION

To obtain potential NS3 helicase inhibitors from extracts of marine organisms, we performed photoinduced electron transfer (PET)-based high-throughput screening.[21] From 23 extracts of marine organisms, number 2 significantly decreased the activity of NS3 helicase (Table S1, Supporting Information), suggesting the presence of a potential NS3 helicase inhibitor. The presence of **1**[16] was identified in sample 2 by comparing its NMR spectra with those previously reported for **1**.[22] We then examined the activity of commercially available **1** against NS3 helicase. We found that the inhibition of NS3 helicase activity by **1** corresponded to that seen with the extract, indicating that **1** provides the main helicase inhibitory activity of sample 2 (data not shown).

To confirm the inhibitory activity of **1** against NS3 helicase, we examined the effect of **1** in an RNA helicase assay using ^{32}P-labeled dsRNA as a substrate. As shown in Figure 1A, **1** inhibited the dsRNA unwinding, with an approximate IC_{50} value of 15 μM.

To determine the effect of **1** on ATPase activity of NS3, we measured the released inorganic phosphate from radioisotope-labeled ATP. The hydrolysis of ATP catalyzed by NS3 was inhibited in a dose-dependent manner by **1** (Figure 1B and C) with an IC_{50} value 70 μM. Next, we examined the effects of **1** at varying ATP concentrations with fixed amounts of NS3 (300 nM) and poly(U) RNA (0.1 μg/μL) to determine whether **1** competes with ATP for the same binding site on NS3. The Lineweaver–Burk equation was used to determine K_m value in the presence and absence of **1**. In Figure 2, the intercepts of the x-axis and the y-axis on the Lineweaver–Burk double reciprocal plot indicate $-1/K_m$ and $1/V_{max}$, respectively. The Lineweaver–Burk double reciprocal plot showed that the apparent K_m value was not changed by **1**. In contrast, V_{max} was altered in the presence of **1**. These data indicate that **1** exhibits noncompetitive-type inhibition.

We also determined the effects of **1** on the ATPase activity of human DHX36/RHAU, a putative RNA helicase whose ATPase activity is required for mRNA deadenylation and degradation.[23] Manoalide (**1**) inhibited the ATPase activity of DHX36/RHAU at the same concentration of **1** required to inhibit the ATPase of NS3 (Figure 3A). Both proteins belong to superfamily 2 (SF2), and they share a catalytic core with high structural similarity to a helicase motif (Figure 3B).[24] Our results suggested that **1** binds to the conserved helicase motif and interferes with the ATPase of helicases.

As binding of NS3 to single-stranded regions of substrate RNA is required for its unwinding activity, we tested whether **1** inhibits the binding of NS3 to ssRNA. We employed a gel mobility shift assay (GMSA) to determine the binding activity of NS3 to human lethal-7 (let-7) microRNA precursor ssRNA. We found that NS3 binding to ssRNA was inhibited by **1** (Figure 4, lane 4). Because poly(U) RNA enhances the ATPase activity of NS3,[25] there is a possibility that the inhibition of NS3 ATPase activity by **1** is caused by inhibition of poly(U) RNA binding. To test this possibility, we performed an ATPase assay in the absence of poly(U) RNA (Figure 5). ATPase activity of NS3 was inhibited by **1** in the absence of poly(U) RNA, ruling out this possibility.

Drugs targeting the unwinding activity could act via one or more of the following mechanisms:[26] (a) inhibiting ATPase activity by interfering with ATP binding and therefore limiting the energy available for the unwinding, (b) inhibiting ATP hydrolysis or release of ADP by blocking opening or closing of domains, (c) inhibiting RNA (or DNA) substrate binding, (d) inhibiting unwinding by sterically blocking helicase translocation, or (e) inhibiting coupling of ATP hydrolysis to unwinding. This study shows that **1** inhibits the ATPase and RNA binding capability of NS3, suggesting that **1** may possess two modes of inhibitory action on NS3 activity. Structural analysis of NS3 revealed that the regions contacting the substrate RNA binding domain and the ATP binding domain are located on opposite faces and are not close to each other.[27] As **1** is a small molecule, it cannot simultaneously mask the RNA binding domain and ATP binding domain. Therefore, we speculate that **1** binds to a certain core helicase motif and interferes with the ATPase through a structural change of the helicase domain (Figure 6 and Figure S1, Supporting

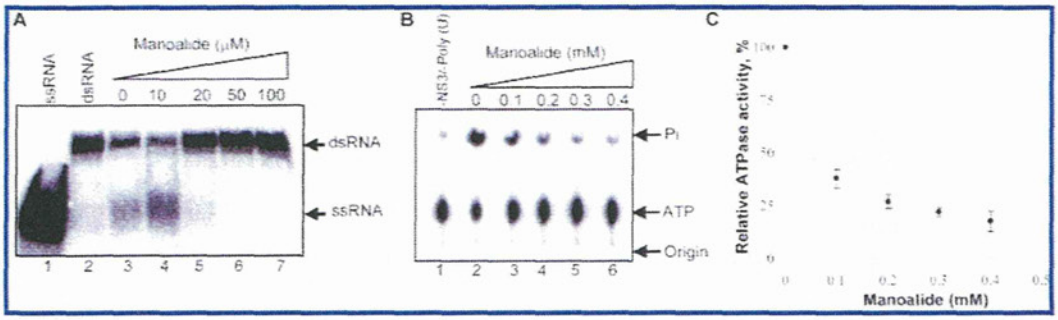

Figure 1. Inhibition of NS3 helicase and ATPase activity by manoalide. (A) The inhibitory effect of manoalide on NS3 helicase activity was determined as described in the Experimental Section. Lane 1 shows the heat-denatured ssRNA (26-mer), and lane 2 shows the partial duplex RNA substrate. Lanes 3–7 show the reactions containing NS3 (300 nM) with increasing concentrations of manoalide (lane 3, 0 μM; lane 4, 10 μM; lane 5, 20 μM; lane 6, 50 μM; lane 7, 100 μM). (B) The reaction mixtures were incubated with [γ-^{32}P] ATP as described in the Experimental Section. Lane 1 contains a control reaction mixture in the absence of NS3 and poly(U) RNA. Lane 2 shows the reaction mixture containing only NS3 (300 nM) and 5% DMSO. Lanes 3–6 show the NS3 reaction with increasing concentrations of manoalide (lane 3, 0.1 mM; lane 4, 0.2 mM; lane 5, 0.3 mM; lane 6, 0.4 mM).The origin, migration of input ATP, and NS3-hydrolyzed inorganic phosphate (Pi) are indicated on the right side of the figure. (C) The experiment shown in panel B is represented graphically. Hydrolytic activity in the absence of inhibitor was taken as 100%. Experiments were conducted independently three times, and their means ± standard deviations were included at each point. An IC_{50} of manoalide of 70 μM was calculated from this figure.

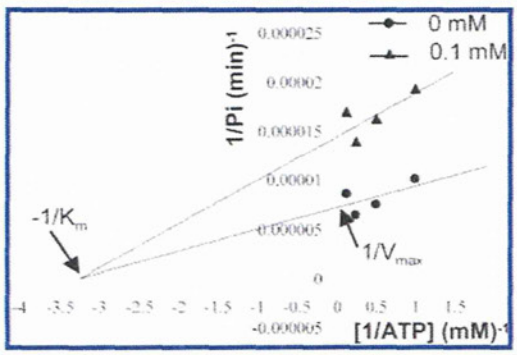

Figure 2. Kinetic profile of manoalide on the inhibition of NS3 ATPase activity. Reactions were performed in 25 mM MOPS–NaOH (pH 7), 1 mM DTT, 5 mM $MgCl_2$, 5 mM $CaCl_2$, 300 nM NS3, and 0.1 μg/μL poly(U) RNA at various [γ-^{33}P] ATP concentrations (1, 2, 4, and 8 mM) in the presence of the indicated concentrations of manoalide (0 mM manoalide, filled circles; 0.1 mM manoalide, filled triangles).

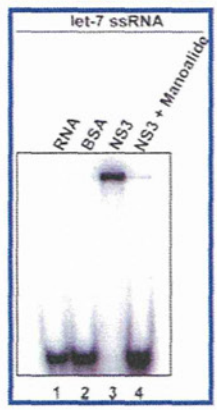

Figure 4. Gel mobility shift assay for the inhibition of NS3 RNA binding. GMSA was performed as described in the Experimental Section. Lanes 1–4 show the GMSA with 1 nM labeled let-7 ssRNA. Heat-denatured RNA alone (lane 1), 300 nM BSA (lane 2), 300 nM NS3 (lane 3), 300 nM NS3 + 0.1 mM manoalide (lane 4).

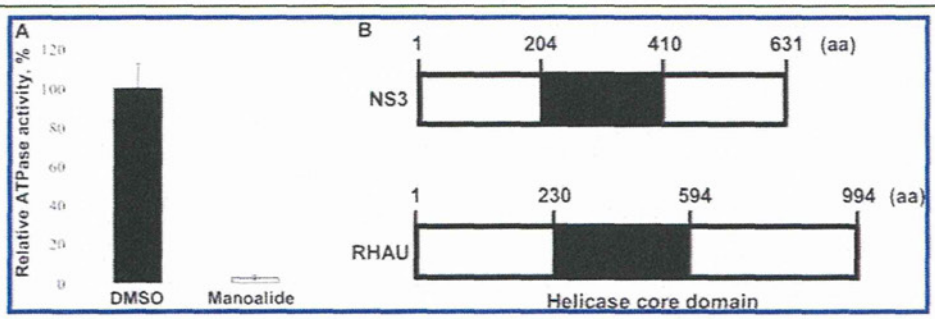

Figure 3. Inhibition of DHX36/RHAU ATPase activity. (A) Reactions were incubated in a buffer solution (50 mM MOPS [pH 7], 2 mM DTT, 3 mM $MgCl_2$) containing 0.5 μL of RHAU, 0.1 μg/μL poly(U) RNA, 0.1 mM manoalide, and 0.1 mM [γ-^{32}P] ATP at 37 °C for 30 min. Black and white bars indicate reactions performed in the absence (5% DMSO) or presence of manoalide, respectively. The data are means ± standard deviations of triplicate assays. (B) Schematic overview of NS3 and RHAU structures. Sequence alignment was carried out on CLUSTALW (http://www.genome.jp/tools/clustalw/). Black box indicates the helicase core domain conserved in SF2 helicases. The numbers indicate amino acid residues.

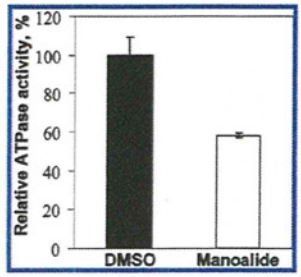

Figure 5. Effects of manoalide on NS3 ATPase activity in the absence of poly(U) RNA. Reaction mixtures contained 25 mM MOPS–NaOH (pH 7), 1 mM DTT, 5 mM $MgCl_2$, 5 mM $CaCl_2$, 600 nM NS3, and 0.1 mM manoalide. These were incubated with 1 mM [γ-^{32}P] ATP in the absence of poly(U) RNA at 37 °C for 60 min. Black and white bars indicate that the reactions were performed in the absence (5% DMSO) or presence of manoalide, respectively. The data are means ± standard deviations of triplicate assays.

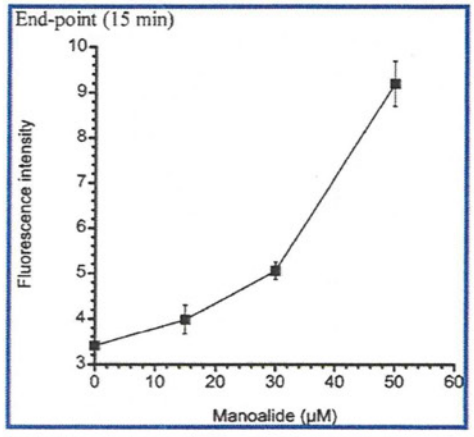

Figure 6. Isothermal denaturation assay (ITD). The ITD assay was performed in 25 mM MOPS–NaOH (pH 6.5), 10× concentrated SYPRO orange, and 240 nM NS3 helicase in 20 μL of reaction mixture with the indicated increasing concentrations of manoalide. The data are means ± standard deviations of triplicate assays.

Information). To test this idea, we have carried out an isothermal denaturation (ITD) assay, which can assess the stability of proteins at temperatures below the melting temperature and detect the binding of ligands.[28] The ITD assay was employed by detecting the increase of fluorescence intensity with the structural change of NS3 as described previously.[29] Figure 6 shows that the fluorescence intensity increased in a dose-dependent manner, strongly suggesting that the NS3 structure was changed by the addition of **1**. This result supports the idea that **1** inhibits NS3 activities through the structural changes by direct binding.

Manoalide (**1**) was originally isolated as an inhibitor of betabungarotoxin and phospholipase A_2[30] but was later found to inhibit calcium channels[18] and 5-lipoxygenase.[19] The hemiacetal in the dihydropyran ring of **1** has been shown to be required for the inhibition of phospholipase A_2.[31] So far, we do not know if the hemiacetal is also essential for the inhibition of NS3. We speculate that acetal formation between a hemiacetal residue of **1** and a serine and/or threonine residue of the helicase core domain, which contains many evolutionally conserved serine and threonine residues, may occur. Future structural and functional analyses will reveal the essential structure of **1** required to inhibit NS3, allowing the development of specific inhibitors to NS3 but not phospholipase A_2.

EXPERIMENTAL SECTION

Preparation of Extracts from Marine Organisms. Specimens of marine sponges were collected in Okinawa, Japan (Table S1, Supporting Information). The specimens were extracted three times with either EtOH or acetone, and the EtOAc-soluble portions were obtained after concentration and partition.

Chemicals. Manoalide was purchased from Santa Cruz Biotechnology. γ-^{32}P-ATP and γ-^{33}P-ATP were purchased from Muromachi Yakuhin and PerkinElmer, respectively. Let-7 ssRNA was synthesized by Gene Design Inc. Poly (U) RNA was obtained from Sigma-Aldrich.

High-Throughput Screening of NS3 Helicase Inhibitors. The fluorescence helicase activity assay based on photoinduced electron transfer was performed as described in our previous study[21] with modifications of the substrate and the composition of the reaction mixture.

The substrate was prepared as dsRNA by annealing, at a 1:2 molar ratio, a 5′ BODIPY FL-labeled 37-mer (5′-CUAUUACCUCCACCCUCAUAACCUUUUUUUUUUUUUU-3′) to a 23-mer (GGUUAUGAGGGUGGAGGUAAUAG). When unwound by HCV NS3 helicase, the unlabeled ssRNA is captured by a DNA capture strand (5′-CTATTACCTCCACCCTCATAACC-3′). A fluorescent-dye-labeled oligonucleotide was purchased from J-Bio 21 Corporation. BODIPY FL was attached to the 5′-end via an aminohexylphosphate linker with a six-carbon spacer. Unlabeled oligonucleotides were purchased from Japan Bio Services Co., Ltd.

The continuous fluorescence assay was performed in 25 mM MOPS–NaOH (pH 6.5), 3 mM $MgCl_2$, 2 mM DTT, 4 U RNasin (Promega), 50 nM dsRNA substrate, 100 nM DNA capture strand, and 5 mM ATP in 20 μL of reaction mixture. The diluted extracts in DMSO were added (2 μL) to the reaction mixtures to a final concentration of 15–35 μg/mL. The reaction was started by adding 240 nM HCV NS3 helicase, which was expressed and purified as described previously,[21] and performed at 37 °C for 30 min using a LightCycler 1.5 (Roche). The fluorescence intensity was recorded every 5 s from 0 to 5 min and then every 30 s from 5 to 30 min. The activity of NS3 helicase was calculated as the initial reaction velocity. Inhibition was calculated relative to the control value examined without inhibitors but with DMSO.

ATPase Assay. NS3 ATPase activity was directly determined by monitoring [γ-^{32}P] ATP hydrolysis by thin-layer chromatography. The assays were performed as previously described[32] with slight modifications. Unless otherwise specified, the standard assay mixture contained 25 mM MOPS–NaOH (pH 7.0), 1 mM DTT, 5 mM $MgCl_2$, 5 mM $CaCl_2$, 1 mM [γ-^{32}P] ATP (PerkinElmer), 300 nM NS3, and 0.1 μg/μL poly(U) with the indicated increasing concentrations of manoalide in a reaction volume of 10 μL. Reactions were conducted at 37 °C for 10 min and stopped by the addition of stop solution (10 mM EDTA). A 2 μL amount of each reaction mixture was spotted onto polyethyleneimine cellulose sheets (Merck) and developed in 0.75 M LiCl/1 M formic acid solution for 20 min. The cellulose sheets were dried, and released [^{32}P] phosphoric acid was visualized with an FLA-9000 image reader and quantified by Multi Gauge V3.11 software (Fujifilm).

RNA Binding Assay. RNA binding was determined by a gel mobility shift assay.[33] First, let-7 ssRNA (5′-UGAGGUAGUAGGUUGUAUAGU-3′) was labeled at the 5′-end with [γ-^{32}P] ATP (Muromachi) using T4 polynucleotide kinase (Toyobo) at 37 °C for 60 min and purified by the phenol-chloroform extraction method. Each 20 μL of reaction mixture contained 30 mM Tris-HCl (pH 7.5), 100 mM NaCl, 2 mM $MgCl_2$, 1 mM DTT, 20 units of RNasin Plus (Promega) that was incubated with 300 nM NS3, 1 nM let-7 labeled ssRNA, and 0.1 mM manoalide at room temperature for 15 min. An equal volume of dye solution [0.025% bromophenol blue, 10% glycerol in 0.5× Tris/borate/EDTA (TBE)] was added to each reaction mixture and loaded onto a 6% native-PAGE gel

dx.doi.org/10.1021/np200883s | J. Nat. Prod. 2012, 75, 650–654

(acrylamide:bis = 19:1). The labeled RNA bands were visualized with an FLA-9000 image reader (Fujifilm).

RNA Helicase Assay. The NS3 RNA helicase assay was performed as described previously[32] with some modifications. Briefly, the substrate for annealing two complementary RNA oligonucleotides, 5′-AGAGAGAGAGGUUGAGAGAGAGAGUUUGAGAGAGA-GAG-3′ (40-mer, template strand) and 5′-CAAACUCUCUCUCU-CUCAACAAAAAA-3′ (26-mer, release strand), was purchased from Shanghai GenePharma Co., Ltd. The release strand was labeled at the 5′-end with [γ-^{32}P] ATP (Muromachi) using the T4 polynucleotide kinase (Toyobo) at 37 °C for 60 min and purified by phenol-chloroform extraction. The template and the labeled release strands were annealed at a molar ratio of 3:1 (template/release), denatured at 80 °C for 5 min, and slowly renatured at 23 °C for 30 min in an annealing buffer [20 mM Tris-HCl (pH 8), 0.5 M NaCl, 1 mM EDTA]. The partial duplex RNA substrate was purified on a G-50 microcolumn (GE Healthcare) and stored at −20 °C in H_2O containing 0.25 U of RNasin Plus (Promega) per μL.

The inhibition assay of NS3 RNA helicase activity by manoalide was conducted in 20 μL of helicase reaction mixture [25 mM MOPS−NaOH (pH 7), 2.5 mM DTT, 2.5 U of RNasin Plus (Promega), 100 μg of BSA per mL, 3 mM $MgCl_2$] containing 300 nM NS3 protein and 0.4 nM ^{32}P-labeled partial duplex RNA substrate with increasing concentrations of manoalide (as indicated) and preincubated at 23 °C for 15 min. After adding 5 mM ATP, the reaction was carried out at 37 °C for 30 min and stopped by adding 5 μL of helicase termination buffer (0.1 M Tris [pH 7.5], 20 mM EDTA, 0.5% SDS, 0.1% Nonidet P-40, 0.1% bromophenol blue, 0.1% xylene cyanol, 25% glycerol). The inhibition of NS3 helicase activity was analyzed on a 10% native TBE polyacrylamide gel, and the labeled RNAs were visualized with an FLA-9000 image reader (Fujifilm).

Isothermal Denaturation Assay. The effect of manoalide on the structure change of NS3 helicase was measured using the isothermal denaturation assay.[29] Briefly, the ITD assay was performed in 25 mM MOPS−NaOH (pH 6.5), 10× concentrated SYPRO orange (Molecular Probes, Eugene, OR, USA), and 240 nM NS3 helicase in 20 μL of reaction mixture with the indicated increasing concentrations of manoalide (Santa Cruz Biotechnology). While SYPRO orange has a low quantum yield in an aqueous environment, the fluorescence intensity increases when the dye binds to the hydrophobic regions exposed upon unfolding of the enzyme. The reaction was carried out in three replicates for each concentration of manoalide at 37 °C for 15 min using a LightCycler 1.5 (Roche) with the fluorescence intensity measured.

■ ASSOCIATED CONTENT

Ⓢ Supporting Information

Summary of NS3 helicase inhibitory activity in extracts of marine sponges and Figure S1. This material is available free of charge via the Internet at http://pubs.acs.org.

■ AUTHOR INFORMATION

Corresponding Author

*Phone: +81-3-5841-3057. Fax: +81-3-5841-3049. E-mail: akimitsu@ric.u-tokyo.ac.jp.

Notes

The authors declare no competing financial interest.

■ ACKNOWLEDGMENTS

The authors express gratitude and special thanks to S. Nishikawa (AIST) for his kind gift of the expression plasmid pT7/His-NS3 containing an N-terminal His-tagged full-length HCV NS3.

■ REFERENCES

(1) Gravitz, L. *Nature* **2011**, *474*, S2−S4.
(2) Butt, A. A. *Expert Rev. Anti-Infect. Ther.* **2005**, *3*, 241−249.
(3) Soriano, V.; Peters, M. G.; Zeuzem, S. *Clin. Infect. Dis.* **2009**, *48*, 313−320.
(4) Koziel, M. J.; Peters, M. G. *New Engl. J. Med.* **2007**, *356*, 1445−1454.
(5) Kai, L. *Virol. Sin.* **2010**, *25*, 246−266.
(6) McHutchison, J. G.; Gordon, S. C.; Schiff, E. R.; Shiffman, M. L.; Lee, W. M.; Rustgi, V. K.; Goodman, Z. D.; Ling, M. H.; Cort, S.; Albrecht, J. K. *New Engl. J. Med.* **1998**, *339*, 1485−1492.
(7) Cummings, K. J.; Lee, S. M.; West, E. S.; Cid-Ruzafa, J.; Fein, S. G.; Aoki, Y.; Sulkowski, M. S.; Goodman, S. N. *J. Am. Med. Assoc.* **2001**, *285*, 193−199.
(8) Tam, R. C.; Lau, J. Y.; Hong, Z. *Antiviral Chem. Chemother.* **2001**, *12*, 261−272.
(9) Choo, Q. L.; Kuo, G.; Weiner, A. J.; Overby, L. R.; Bradley, D. W.; Houghton, M. *Science* **1989**, *244*, 359−362.
(10) Takamizawa, A.; Mori, C.; Fuke, I.; Manabe, S.; Murakami, S.; Fujita, J.; Onishi, E.; Anodoh, T.; Yoshida, I.; Oakayama, H. *J. Virol.* **1991**, *65*, 1105−1113.
(11) Moradpour, D.; Penin, F.; Rice, C. M. *Nat. Rev. Microbiol.* **2007**, *5*, 453−463.
(12) De Francesco, R.; Steinkühler, C. *Curr. Top. Microbiol. Immunol.* **2000**, *242*, 149−169.
(13) Raney, K. D.; Sharma, S. D.; Moustafa, I. M.; Cameron, C. E. *J. Biol. Chem.* **2010**, *285*, 22725−22731.
(14) Burney, T.; Dusheiko, G. *Expert Rev. Anti-Infect. Ther.* **2011**, *9*, 151−160.
(15) Bacon, B. R.; Gordon, S. C.; Lawitz, E.; Marcellin, P.; Vierling, J. M.; Zeuzem, S.; Poordad, F.; Goodman, Z. D.; Sings, H. L.; Boparai, N.; Burroughs, M.; Brass, C. A.; Albrecht, J. K.; Esteban, R. *New Engl. J. Med.* **2011**, *364*, 1207−1217.
(16) De Silva, E. D.; Scheuer, P. J. *Tetrahedron Lett.* **1980**, *21*, 1611−1614.
(17) Newman, D. J.; Cragg, G. M. *J. Nat. Prod.* **2004**, *67*, 1216−1238.
(18) Wheeler, L. A.; Sachs, G.; De Vries, G.; Goodrum, D.; Woldemussie, E.; Muallem, S. *J. Biol. Chem.* **1987**, *262*, 6531−6538.
(19) De Vries, G. W.; Amdahl, L.; Mobasser, A.; Wenzel, M.; Wheeler, L. A. *Biochem. Pharmacol.* **1988**, *37*, 2899−2905.
(20) Bennett, C. F.; Mong, S.; Wu, H. L.; Clark, M. A.; Wheeler, L.; Crooke, S. T. *Mol. Pharmacol.* **1987**, *32*, 587−593.
(21) Tani, H.; Akimitsu, N.; Fujita, O.; Matsuda, Y.; Miyata, R.; Tsuneda, S.; Igarashi, M.; Sekiguchi, Y.; Noda, N. *Biochem. Biophys. Res. Commun.* **2009**, *379*, 1054−1059.
(22) Uddin, M. H.; Otsuka, M.; Muroi, T.; Ono, A.; Hanif, N.; Matsuda, S.; Higa, T.; Tanaka, J. *Chem. Pharm. Bull.* **2009**, *57*, 885−887.
(23) Tran, H.; Schilling, M.; Wirbelauer, C.; Hess, D.; Nagamine, Y. *Mol. Cell* **2004**, *13*, 101−111.
(24) Fairman-Williams, M. E.; Guenther, U. P.; Jankowsky, E. *Curr. Opin. Struct. Biol.* **2010**, *20*, 313−324.
(25) Suzich, J. A.; Tamura, J. K.; Palmer-Hill, F.; Warrener, P.; Grakoui, A.; Rice, C. M.; Feinstone, S. M.; Collett, M. S. *J. Virol.* **1993**, *67*, 6152−6158.
(26) Borowski, P.; Deinert, J.; Schalinski, S.; Bretner, M.; Ginalski, K.; Kulikowski, T.; Shugar, D. *Eur. J. Biochem.* **2003**, *270*, 1645−1653.
(27) Gu, M.; Rice, C. M. *Proc. Nat. Acad. Sci. U. S. A.* **2010**, *107*, 521−528.
(28) Senisterra, G. A.; Hong, B. S.; Park, H. W.; Vedadi, M. *J. Biomol. Screen.* **2008**, *13*, 337−342.
(29) Sarver, R. W.; Rogers, J. M.; Stockman, B. J.; Epps, D. E.; DeZwaan, J.; Harris, M. S.; Baldwin, E. T. *Anal. Biochem.* **2002**, *309*, 186−195.
(30) De Freitas, J. C.; Blankemeier, L. A.; Jacobs, R. S. *Experientia* **1984**, *40*, 864−865.
(31) Glaser, K. B.; de Carvalho, M. S.; Jacobs, R. S.; Kernan, M. R.; Faulkner, D. J. *Mol. Pharmacol.* **1989**, *36*, 782−788.
(32) Gallinari, P.; Brennan, D.; Nardi, C.; Brunetti, M.; Tomei, L.; Steinkühler, C.; De Francesco, R. *J. Virol.* **1998**, *72*, 6758−6769.
(33) Huang, Y.; Liu, Z. R. *J. Biol. Chem.* **2002**, *277*, 12810−12815.

臨床検査のガイドライン

JSLM2012

検査値アプローチ／症候／疾患

編集

日本臨床検査医学会ガイドライン作成委員会

日本臨床検査医学会

付　録

JSLM 2012

肝　疾　患

［要　旨］ 肝疾患の病因，病期を的確に診断し，病態に応じた治療を加えることにより病状の進展を阻止する。
フォローアップの目的は，非代償性肝硬変，肝細胞癌，食道静脈瘤破裂など生命に関わる状態への病状進行を早期に発見し阻止することにある。慢性肝疾患の進展に従って肝細胞癌の発生率が増加するため，慢性肝疾患の病状に応じた定期フォローアップが重要となる。

［キーワード］ 肝機能検査，肝細胞癌，慢性肝炎，肝硬変

疑うべき臨床症状

図1に肝疾患を疑う臨床症状や所見および病歴を示す。

急性肝炎：全身倦怠感や微熱などの感冒様症状や吐き気，食欲不振などの消化器症状から発症する。肝障害の程度が強い場合は黄疸やそれに伴う尿の濃染を認める。

慢性肝炎：特に症状を認めないことが多い。肝炎の増悪時には食欲不振や全身倦怠感を伴う。

肝硬変：代償性期では臨床症状に乏しい。微熱，全身倦怠感を認めることがある。手掌紅斑，くも状血管拡張，女性化乳房を認めることがある。非代償期には，腹水，黄疸，下腿浮腫，肝性脳症，下腿浮腫，ばち状指などを認める。

肝細胞癌：初期の肝細胞癌は，無症状であるが，基礎疾患として慢性肝炎，肝硬変など慢性肝疾患を有していることが多いため，基礎疾患に伴う症状を有する。進行肝細胞癌では，腹痛，腹部膨満感を認める。

確定診断に要する検査

肝疾患を疑う自覚症状を認めた場合や健康診断などで肝疾患を疑う検査結果を得た場合には，図1に示したように自覚症状，臨床所見の確認を行うとともに医療面接で詳しく肝疾患に関連する事項について確認する。

A.　肝機能異常のスクリーニング検査

肝細胞障害，胆汁うっ滞，肝予備力，画像診断の4項目をカバーするように検査を行う。黄疸を認める場合の診断フローチャートを図2に，またAST，ALTの異常を認めた場合の鑑別診断上のポイントを表1に示す。

B.　重症度の判定と入院治療か外来治療かの判断

肝障害が検査で確認された場合には，肝予備力などを参考に入院治療の必要性を判断する（表2参照）急性肝障害の場合は，肝性脳症，顕性黄疸，出血時間の延長

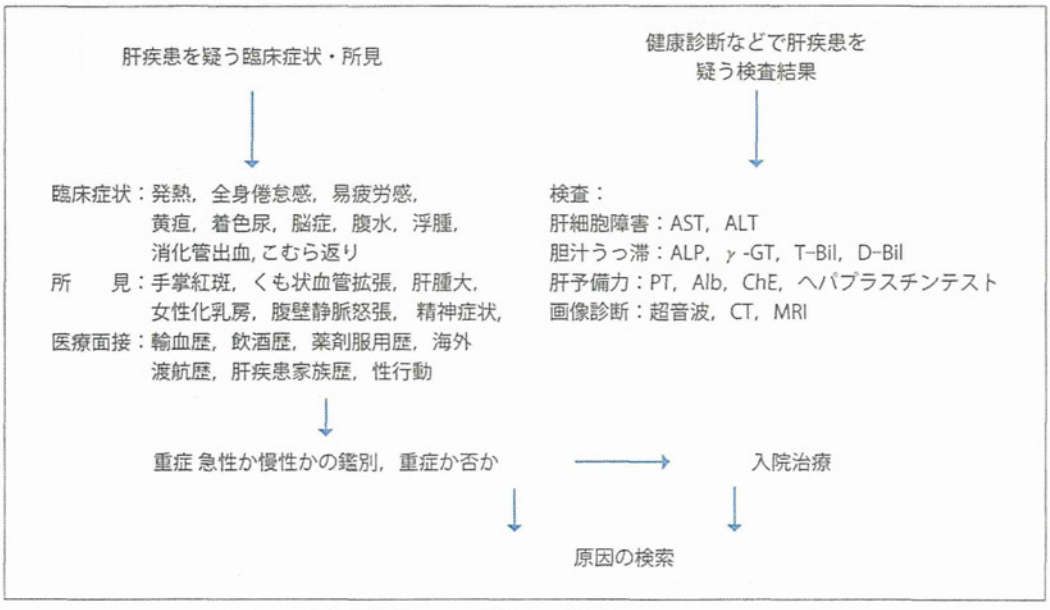

図1　肝疾患が疑われる場合の基本的なフローチャート

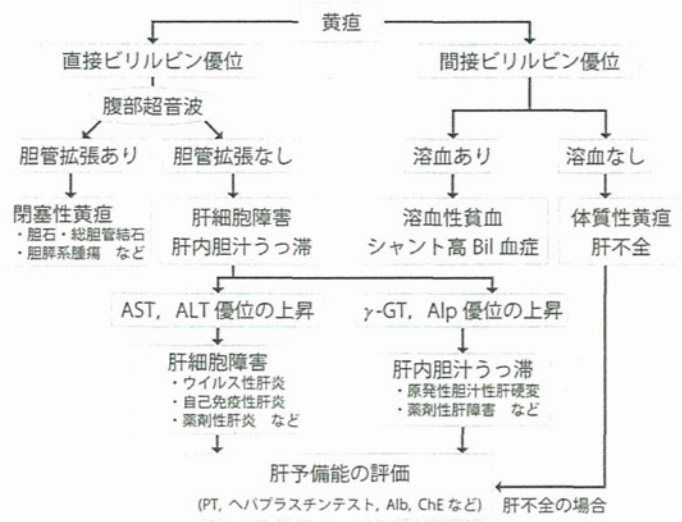

図 2　黄疸を認めた場合の診断フローチャート

表 1 AST, ALT 異常時の鑑別診断上のポイント

➢ 500 U/L 以上
・急性肝炎（ALT>AST，初期は AST 優位）
・劇症肝炎
・ショック肝（LDH も著明に上昇）
➢ 100～500 U/L
・慢性活動性肝炎（ALT>AST）
・薬剤性肝障害（ALT<AST，胆道系酵素の上昇）
・アルコール性肝炎（ALT<AST，γ-GT の上昇）
・胆汁うっ滞（胆道系酵素優位の上昇）
・溶血・心筋梗塞（ALT<AST）
➢ 100 U/L 以下
・慢性肝炎（ALT>AST）
・脂肪肝（脂質異常，糖代謝異常を伴うことが多い）
・肝硬変（ALT<AST，Alb の低下，血小板数の低下）
・うっ血肝（ALT<AST）

表 2　肝障害の際の入院適応

・急性肝炎でまだ回復期に至っていない症例
・慢性肝炎の急性増悪時：外来での治療（経口剤，強ミノ静注など）にもかかわらず AST や ALT が 300～500 U/L 以上となった時
・肝予備能が低下している症例（PT 70%以下）
・初めての顕性黄疸（T-Bil>2 mg/dL）の出現時または黄疸の急激な進行
・肝硬変患者で初めての肝性脳症，腹水の出現時
・外来での塩分制限や投薬などにてコントロールのつかない肝性脳症や腹水
・腫瘤性病変の疑われた時
・食道静脈瘤の出血時およびその治療のため
・インターフェロンなど積極的な治療開始のため
・肝生検・腹腔鏡など検査入院
・その他（慢性肝炎や肝硬変の自覚症状が特に強い時など）

など予備能の大幅な低下がある場合は，入院で加療する。生命に関わる食道静脈瘤からの出血や肝細胞癌の有無により判定する。

C.　病因の鑑別

表 3 に鑑別すべき疾患と診断上ポイントとなる検査項目を示す。

1)　ウイルス性肝炎

急性肝炎を惹起するウイルスには，A 型，B 型，C 型，E 型の肝炎ウイルスが存在する。それぞれのウイルスマーカーにより鑑別する。A 型肝炎は生牡蠣など貝，カニの経口摂取により感染する。IgM-HA 抗体が診断に有用である。B 型肝炎は，血液を介してもしくは性的接触により感染する。B 型肝炎関連ウイルスマーカーの測定を行う。C 型肝炎は，血液を介する感染が主体である。E 型肝炎は，国内では猪肉や鹿肉などの摂取による感染事例があり人畜共通感染症である。南アジア，東南アジアなど海外からの輸入感染症であることも多い。

2)　アルコール性肝障害

飲酒状況の詳細な把握が最も重要である。日本酒換算で一日 3 合以上を 5 年以上継続している常習飲酒家に起こることが多い。トランスアミナーゼは AST>ALT で上昇し，γ-GT の上昇を伴う。MCV の上昇も参考になる。禁酒により肝機能が改善することが確定診断につながる。

3)　自己免疫性肝障害

自己免疫性肝炎（AIH），原発性胆汁性肝硬変（PBC），原発性硬化性胆管炎（PSC）がある。自己免疫性肝炎は中年女性に多く，トランスアミナーゼ（AST，ALT）の上昇が主体で，γ グロブリンや血清 IgG が 2000 mg/dL を超えることが多い。抗核抗体，抗平滑筋抗体，肝腎ミクロソーム抗体などの自己抗体が陽性になることが多い。PBC も中年女性に多く，ALP，γ-GT など胆道系酵

表 3　肝障害の原因と鑑別診断に有用な検査

- A 型肝炎：IgM-HA 抗体，IgM，異型リンパ球
- B 型肝炎：HBs 抗原，HBc 抗体，IgM HBc 抗体，HBV-DNA
- C 型肝炎：HCV 抗体，HCV-RNA
- E 型肝炎：HEV-RNA, IgA(IgM)-HEV
- EB ウイルス感染（伝染性単核球症）：EB-VCA IgM 抗体，異型リンパ球
- サイトメガロウイルス感染：CMV IgM 抗体，CMV antigenemia
- アルコール性肝障害：飲酒歴，γ-GT, IgA, MCV
- 自己免疫性肝炎：IgG,γ- グロブリン，抗核抗体，抗平滑筋抗体，抗 LKM 抗体，HLA-DR（保険適応外）
- 原発性胆汁性肝硬変：IgM,γ- グロブリン，抗ミトコンドリア抗体，抗ミトコンドリア M2 抗体
- 脂肪肝：BMI，腹部 US
- NASH：FOMA-R, AST＞ALT, PLT 減少，腹部 US
- 薬物性肝障害：薬物歴，WBC，好酸球数，IgE, DLST
- 胆管閉塞（腫瘍，胆石による）：腹部 US，腹部 CT, MRC
- 甲状腺機能異常：fT4, fT3, TSH
- 心不全（shock liver）：病歴，LDH
- うっ血肝：病歴，腹部 US，心機能
- ウイルソン病：セルロプラスミン，尿中銅，血中銅
- 高シトルリン血症：アンモニア，アミノグラム
- ヘモクロマトーシス：血清鉄，血清フェリチン，トランスフェリン飽和率

素の上昇が主体である。抗ミトコンドリア抗体（AMA）が陽性になること，IgM の上昇が特徴的である。PSC では，ALP を主体とした胆道系酵素の上昇が特徴であるが，AMA は陰性である。診断は ERCP，MRC での特徴的胆管像の確認や肝生検で行う。

4）　脂肪性肝疾患

肝細胞に中性脂肪が過剰に蓄積した状態の肝臓を脂肪性肝疾患と総称し，単純性脂肪肝と NASH に分けられる。いずれも，ウイルス性肝疾患，自己免疫性肝疾患の否定とアルコール摂取の否定をした上で，腹部超音波検査，腹部CT検査で肝臓の脂肪沈着を確認する。NASHは，進行すると肝細胞への脂肪沈着が少なくなるので注意が必要である。NASH か単純性脂肪肝かの鑑別は肝生検によりなされ，血液検査のみで判断するのは困難なことが多い。NASH は，肝細胞の壊死，炎症を引き起こし，線維化をきたすため ALT 値，ヒアルロン酸，IV 型コラーゲンが単純性脂肪肝と比較して高値であることが多い。インスリン抵抗性を示す HOMA-R（FBS×血中インスリン/405）や鉄の沈着を示す血清フェリチンも高値を示すことも多い。NASH は，肝硬変から肝細胞癌へと進展することもあるので，それを念頭においたフォローアップが必要である。

5）　薬物性肝障害

薬物性肝障害は，薬物の肝細胞への直接的な毒性による中毒性肝障害と薬物アレルギー性肝障害に 2 分される。

いずれも薬物摂取歴と除外診断で診断する。頻度的には薬物の投与開始後に 2-3 か月以内に発症することが多いが，長期間服用している薬物が原因のこともあり，注意が必要である。

その他，腫瘍や胆石による胆管閉塞，急性心筋梗塞などの心疾患も肝機能障害を引き起こすので注意を要する。

D.　肝生検の適応と禁忌（表 4）

血液検査，腹部 US など比較的低侵襲の検査で診断がつかない場合の診断確定や，肝疾患の進行度評価や治療効果や予後の予測を目的に肝生検を行うことが考慮される。肝腫瘍性病変が疑われる場合で，総合画像診断で診

表 4　肝生検の適応と禁忌

適　応
・肝機能異常の原因検索
・ウイルス性慢性肝疾患の進行度診断
・自己免疫性肝炎，原発性胆汁性肝硬変，原発性硬化性胆管炎の診断
・アルコール性肝障害の進行度診断
・NASH の診断
・薬物性肝障害の診断
・代謝性疾患の診断（ウイルソン病，高シトルリン血症，アミロイドーシス，ヘモクロマトーシス，肝ポルフィリン症等）
・不明熱（AIDS，悪性リンパ腫等）の病因検索
・全身性炎症性疾患，肉芽腫性疾患（サルコイドーシス等）
・肝移植後の拒絶反応の診断
・遺伝性疾患の家族のスクリーニング
禁忌
・著明な出血傾向　・心肺機能不全
・横隔膜ヘルニア　・腹腔内細菌感染
・全身衰弱状態

断が確定されない場合も，US ガイド下の腫瘍生検を検討する。適応は出血などのリスクも考慮して決定する。

病態把握と治療方針の決定

A. B 型肝炎の病態把握と専門医コンサルテーションのポイント

B 型肝炎感染の診断フローチャートを図 3 に示す。HBs 抗原陽性の肝障害を診た場合，HBV 感染による急性肝炎か HBV キャリアからの急性増悪かの鑑別が臨床上極めて重要であり，HBc 抗体の力価が診断上のポイントとなる。HBV の持続染者（HBV キャリア）に対して肝臓専門医へコンサルテーションする際のポイントを図 4 に示す。HBV-DNA 高値かつ ALT 異常値例あるいは非若年者は肝発癌リスクが高いため肝臓専門医へのコンサルテーションが望ましい。このうち，ALT 異常値を呈する症例は基本的に抗ウイルス療法の適応となる。抗ウイルス療法の目的は，B 型肝炎ウイルスの活動性の低下による ALT の正常化で，肝硬変・肝細胞癌への進展を抑制することである。最近では HBs 抗原の陰性化を最終的な治療目標と考えることが多い。抗ウイルス療法は，インターフェロン投与と核酸アナログ製剤内服に

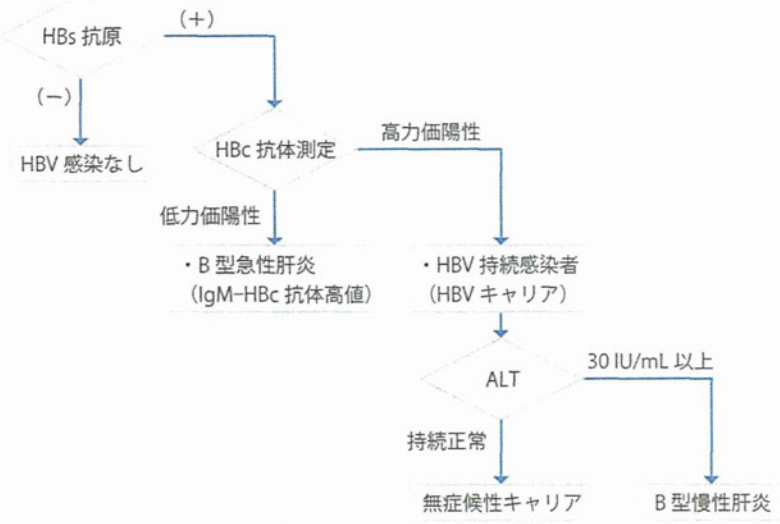

図 3　HBV 感染の診断の流れ

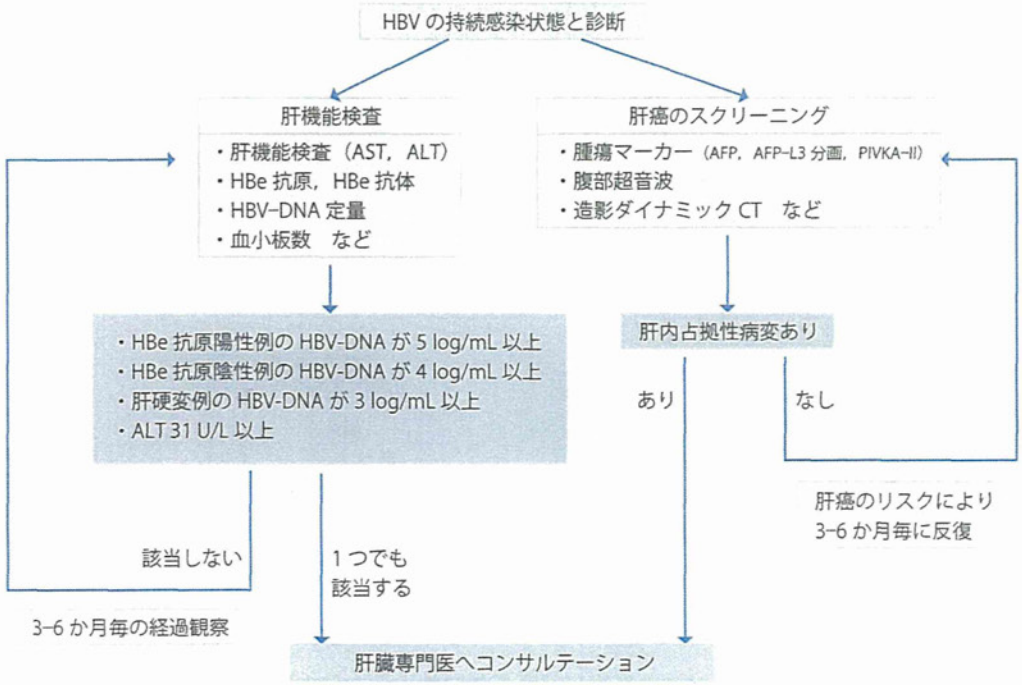

図 4　HBV キャリアを肝臓専門医へコンサルテーションする際のポイント（抗ウイルス療法の適応と発癌リスクを考慮したフローチャート）

よる治療がある。一方，コンサルテーションしない症例でも，定期フォローアップにより肝炎活動性のモニターや肝細胞癌の早期発見につとめることも重要である。

B. C型慢性肝炎の病態把握と専門医コンサルテーションのポイント

C型肝炎感染の診断フローチャートを図5に示す。HCV感染者と診断場合の専門医にコンサルテーションするポイントを図6に示す。ALT31 U/L以上または血小板数15万/μL未満は発癌リスクが高く，抗ウイルス療法の適応であり，肝臓専門医へのコンサルテーションが望ましい。また，慢性肝炎の状態では肝癌が存在しなくてもAFP値の異常を認めることがあるが，AFP 6 ng/mL以上は将来の肝発癌のリスクが高いため，肝臓専門医へのコンサルテーションまたは厳重な経過観察が必要である。C型慢性肝炎の治療の目標は，C型肝炎ウイルスの排除とALTの正常化による，肝硬変と肝癌への進展の抑止である。

C型肝炎に対する抗ウイルス療法は，ウイルス排除を目的とした治療と基本であり，ウイルスのジェノタイプ（あるいはセロタイプ）やウイルス量およびHCV NS5A領域に存在するISDRの遺伝子変異数やHCVコア70番・91番のアミノ酸変異，さらには宿主IL28B遺伝子近傍のSNP等によりその適応を決定する。C型慢性肝炎に対する抗ウイルス療法は，インターフェロンが基本であり，症例に応じてリバビリンやプロテアーゼ阻害剤を併用して行う。

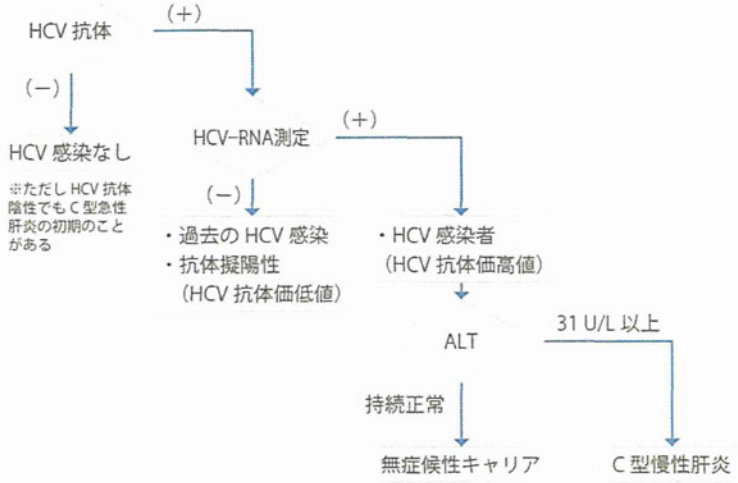

図5　HCV感染の診断の流れ

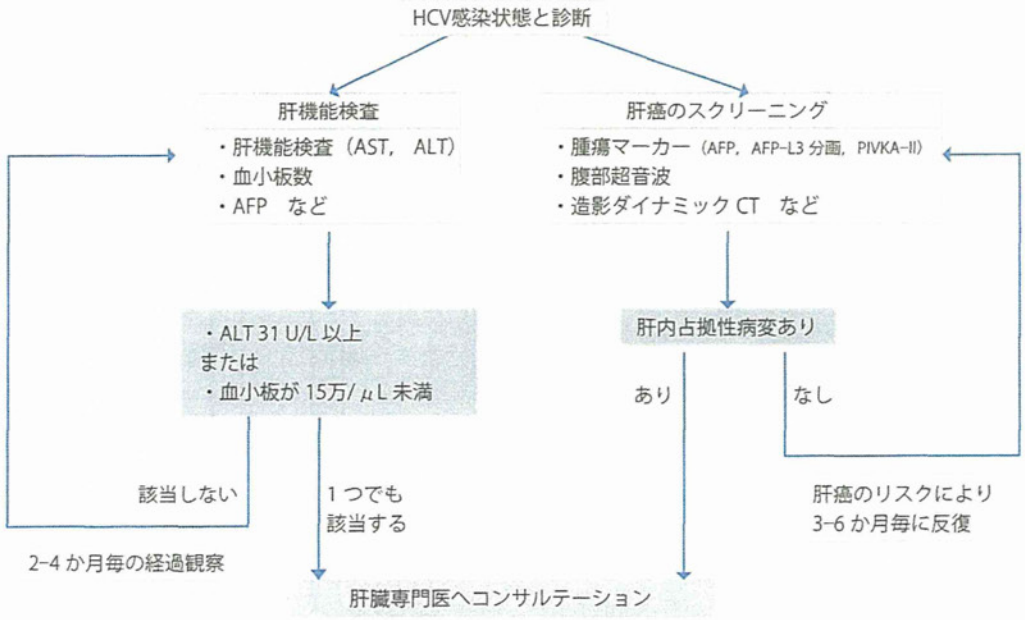

図6　HCVキャリアを肝臓専門医へコンサルテーションする際のポイント
（抗ウイルス療法の適応と発癌リスクを考慮したフローチャート）